Cost effective use of metal oxides/sulphides for Enhanced supercapacitor application

A Thesis Submitted towards Partial Fulfilment

Of BS-MS Dual Degree Programme

By

SUMIT BHATNAGAR

Under the Guidance of

Prof. S.B Ogale, NCL Pune, India

And

Dr. G.V. Pavan Kumar, IISER Pune, India

Department of Chemistry

Indian Institute of Science Education and Research (IISER) Pune

Dedicated to
2009 batch !!!!

Certificate

This is to certify that this dissertation entitled "**Cost effective use of metal oxides/sulphides for Enhanced supercapacitor application**" towards the partial fulfilment of the BS-MS dual degree programme at the Indian Institute of Science Education and Research Pune, represents original research carried out by **Sumit Bhatnagar** at NCL and IISER Pune under the supervision of **Prof. S.B. Ogale**, NCL, pune and **Dr. G.V.Pavan Kumar,** IISER, Pune during the academic year 2013-2014.

Sumit Bhatnagar

Prof. S.B Ogale   **Dr. G.V. Pavan Kumar**

(Supervisor)   (Co-Guide)

Date: Date:

Place: Place:

Prof. K.N. Ganesh

Head (Chemistry)

Date:

Place:

Declaration by the Candidate

I declare that the thesis entitled "**Cost effective use of metal oxides/sulphides for Enhanced supercapacitor application**" submitted by me for the degree of Master of Science for the record of work carried out by me during the academic year 2013-2014 under the guidance of **Prof. S.B Ogale**, NCL Pune and

Dr. G.V. Pavan Kumar, IISER Pune. This work has not formed the basis for the award of any degree, diploma, and fellowship, titles in this or any other University or other institution of higher learning. I further declare that the material obtained from other sources has been duly acknowledged in the thesis.

SUMIT BHATNAGAR

DATE: 2nd APRIL, 2013

PLACE: PUNE

Acknowledgements

I would like to express my gratitude to Professor SatishChandra Ogale for his continuous support and creating an ambience of enthusiasm, motivation and adventure in research. His excellence and unflinching courage in research always inspired and persuaded me to work hard with his noble thoughts. His attitude towards science has not only leaded me to develop as an experimentalist or as a chemist but also to develop a sense of independent thinker.

I would also like to thank my Co-Guide Dr G.V. Pavan Kumar for morally supporting me and inspiring me to achieve excellence in science. He has been a great support for me during my BS-MS. His fantabulous teaching skills really helped me to understand core concepts of the subject.

I would also like to appreciate my lab mates and friends Abhik, Waahid, Rohan, Raunak, Onkar , Dhanya, Divaya, Ketaki, Pradeep, Anirudh, Pooja, Anil, Shruti, Umesh, Aparna, Mukta, Dr. Nilima, Dr.Lily, Yogesh, Dr. Vivek, Dr. Parvej, Dr. Datta, Dr. Sarika, Dr. Mandakini , Kush, Upendra, Aakash, Tanya, Poonam, Ishika and Shrasti for creating an exciting academic atmosphere and supporting me during my failure.

I would also like to acknowledge my teachers from primary school to my college life, without their excellent teaching skills and moral support I would'nt has reached so far.

Lastly I would love to acknowledge my family members and my well wishers without their support and encourangement I wouldn't have able to complete my task.

Contents   **Page number**

List of Figures   Page Number

List of Tables   Page Number

List of Abbreviations

- SEM   Scanning Electron Microscopy
- TEM   Transmission Electron Microscopy
- XRD   X-Ray Diffraction
- NCO   Nickel Cobalt Oxide
- NWs   Nanowires
- CV   Cyclic Voltammetry
- NCS   Nickel Cobalt Sulphide
- EDLC   Electric Double Layer Capacitor

➢ **Abstract**

I report the cost effective use of metal oxides/sulphides for enhanced aqueous based supercapacitor application. The supercapacitive property of the metal oxides and sulfides are generally depends on the conductivity and the surface area. Conductivity is important because it helps the faster electron transfer into the electrode. As the supercapacitor property depends on the available active sites, and so surface area is equally important for enhancement of the capacitive storage property. Higher the surface area, higher will be the atomic active site for the faster reaction. $NiCo_2O_4$ (NCO) is a promising ternary oxide with very high conductivity compared with their corresponding binary oxides. Here we report the synthesis of 1D NCO nanowires as well as high surface area 2D nanosheets and checked the capacitive performance in aqueous KOH electrolyte. Further I have grown Nickel cobalt sulfide nanosheet which possesses higher conductivity than even NCO and checked its performance in same solution.

Introduction

Depletion of conventional energy sources and the need for the reduction of the high amount of CO_2 emitted using these sources have led scientist all over the world to look forward for sustainable energy and clean energy sources such as the electric energy produced by solar and wind based technologies[1]. Hence there is a great need in the 21st century for harnessing of clean renewable energy sources and effective storage of the harnessed energy. To make complete use of these sporadic energy sources we need to work in the development of new and advanced delivery systems and energy storage systems. The storage energy density and power density are two critical parameters which define the effectiveness of energy storage. The energy density defines the quantity of storage energy while power density defines the rate of energy storage and retrieval. One of the main modes of energy storage is the storage of separated charges. In this respect batteries and supercapacitors are the devices at the centre of scientific activity and attention. Batteries support high energy density (at relatively low power density), while supercapacitors render high power density (at relatively low energy density). Their regimes of applicability therefore differ accordingly. Figure (1) shows the comparison between various devices in terms of their energy storage and conversion power. Electrochemical capacitors fill in the gap between conventional capacitors (electrolytic capacitors or metalized film capacitors) which have very low energy density and batteries which have low power density. Thus electrochemical supercapacitors enhance battery performance by providing higher power density or improve the energy density of conventional capacitors when connected with these devices.
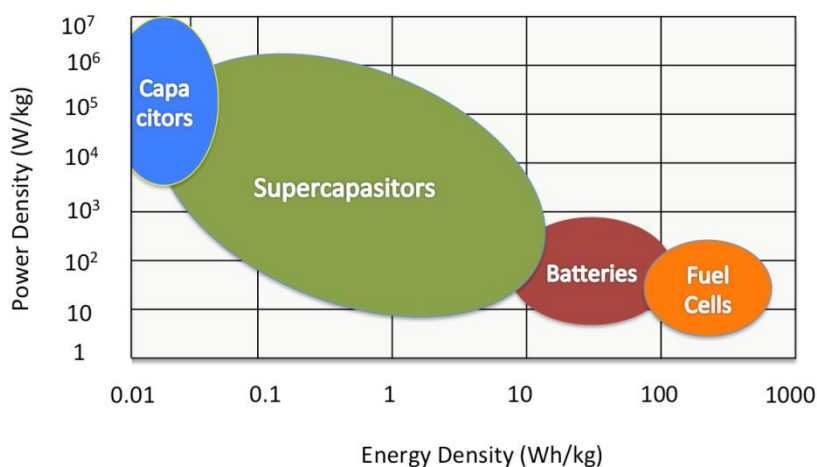

Figure 1: Ragone plot showing relation between energy density and power denstiy

Outstanding properties of supercapcitors make them promising energy storage devices in a wide range of applications, such as hybrid electric vehicles, mobile electronic devices, large industrial equipments, memory backup systems, and military devices, where high power density and long cycle-life are highly desirable.

The quality factors of the batteries and supercapacitor are defined by the materials used and attempts are consistently being made to enhance the energy density of supercapacitors and power density of batteries. Larger surface area and thinner dielectrics (based on conceptually different design alternatives); make the value of capacitance of the supercapacitors significantly higher than the conventional capacitors [1, 2(c)]. Their higher power density, shorter charging time and longer cycle life span than batteries and fuel cells [1, 2(c)] makes them an attractive power solution option for various emergent and futuristic applications.

Figure (2) shows the broad classification of the supercapacitors based on type of the electrode used.
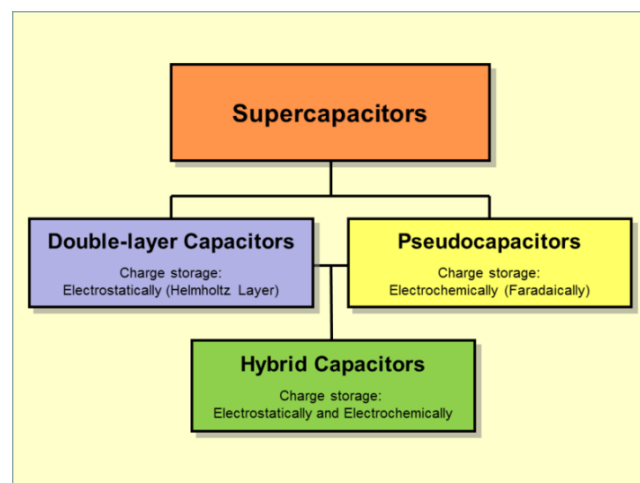
Figure 2: Hierarchical classification of supercapacitors and related types.

Electric Double layer super capacitors (EDLC) stores electric charge by a non faradic mechanism in which electric charge gets stored in the helmontz double layer which is formed at the interface between the electrolyte and the electrode material, due to which charge separation takes place. Capacitance value for EDLC is directly proportional to the surface area of the double layer formed; hence activated carbons with high surface area are used to increase the capacitance for these types of supercapacitors. Figure (3) shows the working mechanism for this type of supercapacitor.
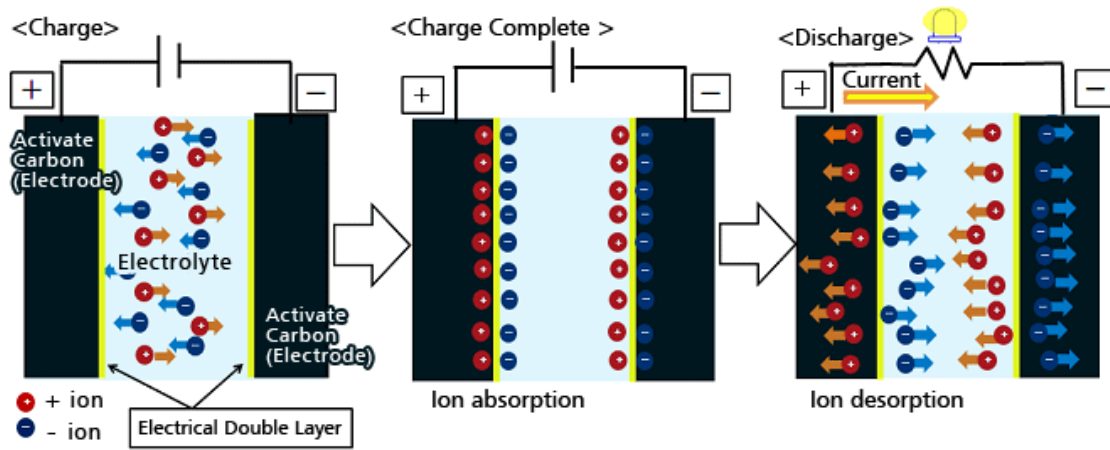
Figure 3: Charge and discharge of EDLC.

Pseudocapacitors store electrical energy by faradic mechanism in which there is a transfer of electrons between electrolyte and the electrode material by redox reactions, electrosorption and intercalation process. Electrode materials of the pseudocapacitors are made up of metal oxides or conducting polymer which offer higher faradic pseudocapacitance than the static double layer capacitor.
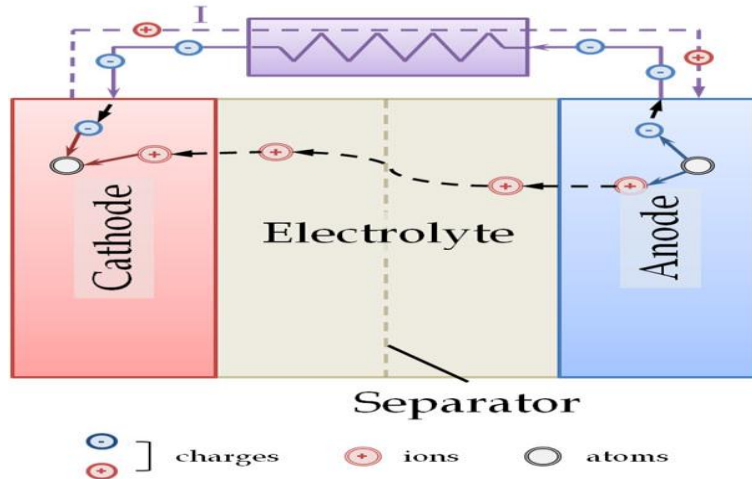
Figure 4: Working mechanism of Pesudocapacitors.

Hybrid Supercapacitors are special type of capacitors in which the electrodes are made such that they offer significant double layer capacitance and pseudocapacitance. In such type of supercapacitors cathode acts as EDLC and anode acts as pseducapacitor. Cathode materials are mostly carbon based materials, while anode materials are mostly metal oxides, conducting polymers.

Supercapacitors formed by such a system are also known as asymmetric supercapacitors. Due to a wide operating potential window for such supercapacitors a much larger energy density can be obtained.

Due to relatively low capacitance of EDLCs, their commercial applications are still limited in cases where high energy is desired. A large energy density is associated with faradic reactions in pseudo-capacitors as compared to EDLC[3]; hence there is growing interest in studying materials systems that are pseudo-capacitive in nature. Different electrode materials such as metal oxides (RuO_2, NiO, Co_3O_4 etc.), nitrides (TiN), sulphides (Co_9S_8, NiS), hydroxides ($Ni(OH)_2$), and conducting polymers (Polyaniline, polypyrole etc) have been examined for supercapacitor applications[4-6]. Amongst them mostly transition metal oxides are being widely studied because of their variable oxidation states, easy chemical synthesis, and ability to store higher amount of energy via proper reversible oxidation-reduction reaction within the potential range of water decomposition[2]. Amongst different transition metal oxides, nickel and cobalt oxides are advantageous because of their low toxicity, higher theoretical capacity, low cost, and their crystal habits which enable realization and control of different shapes and morphologies.

Besides all the binary oxides, ternary oxides are also being studied over the past few years, for their potential advantages over binary oxides in terms of conductivity and fast reversible redox reactions within the broader potential window in aqueous electrolytes. Amongst these, $NiCo_2O_4$ is the most studied ternary oxide for supercapacitor applications because of its low cost[7], easy processability and two orders of magnitude higher conductivity than NiO and Co_3O_4[6]. $NiCo_2O_4$ (NCO) is an inverse spinel, in which nickel occupies tetrahedral sites and cobalt is distributed over both the octahedral and tetrahedral sites. NCO has already been used widely in the fields of magnetism[8], electro-catalysis[9], and electrocatalytic water splitting. It has also been used in devices such as optical limiters and switches[10], chemical sensors[11], and as negative electrode materials in lithium and sodium ion batteries [12, 13]. Recently the ternary NCO is being pursued intensely as an attractive electrode material for supercapacitor applications[6,14-17]. Specifically, morphological modifications of this system have been carried out over the past few years to improve its capacitance behavior. Several methods that have been employed for the synthesis of nickel cobaltite nanoparticles, largely including hydroxide decomposition[17], nanocasting[18], electrodeposition[19], combustion[8], co-precipitation

13

[20], and the sol-gel synthesis[21]. There have been several interesting reports on the synthesis and electrochemical evaluation of $NiCo_2O_4$ nanostructures [6, 15, 22, 23]. For example $NiCo_2O_4$ aerogels synthesized by an epoxide-assisted sol-gel route show highly enhanced electrochemical performance [6]. Also $NiCo_2O_4$ nanowires synthesized through polymer/surfactant-assisted solution method exhibit high capacitance and good cycling ability [15, 22]. Even direct hydrothermal growth of $NiCo_2O_4$ nanostructures on conducting substrates has been carried out to improve the overall capacitance and rate capability, but it has relatively less commercial applicability due to its limited volumetric capacitance. Even in powdered form of NCO, higher capacitance at very low current density has been achieved but problems still to be solved are capacity retention after long cycling and at higher current density. Studies are still ongoing to synthesize different heterostructures to enhance the electrochemical properties of this material system by simple, inexpensive and scalable synthetic strategies to facilitate its use in real commercial applications.

I have reported here, the increase in specific capacitance of electrochemical super capacitors by changing the morphology and conductivity of the electrode material.

1. Facile synthesis of porous $NiCo_2O_4$ nanowires ensemble hierarchical structure for supercapacitor applications.

I report the synthesis of $NiCo_2O_4$ nanowires with unique porous morphology under mild hydrothermal conditions and evaluation of the corresponding electrode for supercapacitor application. We obtain a specific capacitance of 840 F/g at a current density of 4 A/g and it is decreased by 37% as the current density is increased from 2 A/g to 40 A/g. While the growth of $NiCo_2O_4$ nanowires has been accomplished by different synthetic procedures [24-28] mostly a direct deposition method is employed to deposit $NiCo_2O_4$ on different substrates. Our synthetic technique is advantageous because $NiCo_2O_4$ is obtained in a bulk amount, which facilitates in increasing the loading of the electrode material in a smaller area, thereby increasing its volumetric capacitance. This increases commercial application potential of our material. Moreover, our material, because of its unique morphology and microstructure, shows higher or comparable specific capacitance (840 F/g at 4 A/g) than various reports. For instance, synthesis of nanostructured $NiCo_2O_4$/carbon cloth electrode [25] exhibits specific capacitance of 245 F/g at current density of 1 A/g, $NiCo_2O_4$ nanowires

synthesized via facile polyethylene glycol directed technique[22] show a specific capacitance of 743 F/g at current density of 1 A/g, mesoporous $NiCo_2O_4$ nanowires obtained by template-free strategy[26] show a capacitance of 401 F/g at current density of 1 A/g etc. Also while the capacitance value is comparable to other reports, the cyclability of the as-synthesized NCO nanowire-assembled porous nanostructure is superior to most reports.

1.1 Experimental Section

Nickel nitrate hexahydrate ($Ni(NO_3)_2.6H_2O$), cobalt nitrate hexahydrate ($Co(NO_3)_2.6H_2O$) and Triton X-100 were purchased from Merck. Urea was purchased from Sigma Aldrich. All chemicals were of analytical grade and were used without any further purification. In a typical procedure, a mixture of 40 ml solution of 8 mmol of $Co(NO_3)_2.6H_2O$ and 4 mmol of $Ni(NO_3)_2.6H_2O$ was added drop-wise to 40 ml of 4 mmol of Triton X-100 aqueous solution, and after stirring for 1 hour, 16 mmol of urea was added. The mixture was subsequently stirred for additional 3 hours. The solution was then transferred to Teflon lined stainless steel autoclave of 100 ml capacity and was subjected to heating at $120°C$ for 24 h. After cooling the autoclave to room temperature, a light pink solid precipitate was observed which was separated by centrifugation at 10000 rpm with successive repeated washings with water, ethanol-water and pure ethanol. The precipitate was dried at $60°C$ in vacuum, and then annealed at $300°C$ at a heating rate of $1°C/min$. After cooling it down to room temperature, black-colored $NiCo_2O_4$ powder was obtained which was subjected to further characterizations and electrochemical measurements.

1.2 Characterization

Powder X-ray diffraction (XRD) pattern was recorded using Philips X'Pert PRO by Cu K_α radiation. Electron microscopy was performed with FE-SEM (Hitachi S-4200) and HR-TEM (HR-TEM, FEI Tecnai 300). All the electrochemical measurements were conducted in three electrode assembly. The composite electrode was made up by slurry of appropriate amount of active material ($NiCo_2O_4$), conductive additive (Super P), binder (Polyvinylidene fluoride) and 1-methyl-2-pyrrolidinone (NMP) with ratio of 8:1.5:0.5. The slurry was then coated on one side of graphite electrode and dried at $60°C$ for 12 hours. The graphite electrode coated with slurry of $NiCo_2O_4$ served as working electrode, while a platinum strip and Ag/AgCl (saturated KCL)

served as counter and reference electrodes, respectively. All the experiments were carried out using freshly prepared 2M KOH solution. The electrochemical impedance measurement was performed between 0.1 and 10^5 Hz with the voltage amplitude of 5mV.

1.3 Results and discussion:

Uncalcined nickel cobalt hydroxide carbonate was first synthesized in a teflon-lined stainless steel autoclave at $120°C$ for 24 hours with a solution of $Ni(NO_3)_2.6H_2O$, $Co(NO_3)_2.6H_2O$ and Triton-X100 in water. Successive hydroxylation and decomposition of urea at elevated temperature in aqueous solution releases OH^- and CO_3^{2-}, which initiate the precipitation of nickel cobalt hydroxide carbonate species. $NiCo_2O_4$ was then obtained by annealing the nickel cobalt hydroxide carbonate at $350°C$ for 2 hours.

The reactions in the system can be expressed as:

$$NH_2CONH_2 \implies NH_4^+ + NCO^-$$
$$NCO^- + 3H_2O \implies HCO_3^- + NH_4^+ + OH^-$$
$$3HCO_3^- \implies CO_3^{2-} + H^+$$
$$2Co^{2+} + Ni^{2+} + CO_3^{2-} + OH^- \implies \text{Nickel cobalt hydroxide carbonate}$$

$$\text{Nickel cobalt hydroxide carbonate} \xrightarrow{350°C} NiCo_2O_4$$
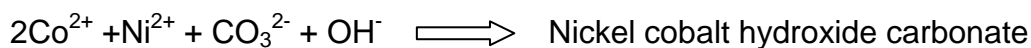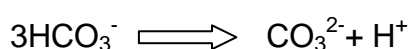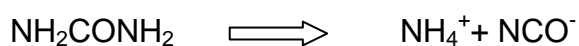
Better structural control and crystallization can be achieved by slow rate of hydrolysis under hydrothermal condition. Experimental parameters which influence the hydrolysis rate and control the nucleation as well as crystal growth processes, such as concentration of metal salt solution, urea, reaction temperature and time[31] were carefully optimized for the reproducible formation of $NiCo_2O_4$ nanowires with the desired morphology and properties. In this work, the role of Triton X-100 is to generate assembled hierarchical nanowire structure. Various factors such as Van der waal forces, hydrophobic interactions, hydrogen bonding, and intrinsic crystal contraction contribute to the final morphology of the material[32].

Figure (5) shows a characteristic powder x-ray diffraction (PXRD) pattern of $NiCo_2O_4$ with d-values at 4.66A°, 2.33A°, 2.85A°, 2.017A°, 1.55A°, 1.42A°, assigned to the planes (111), (220), (311), (400), (511), (440), respectively, of the nanostructured

cubic type $NiCo_2O_4$. Absence of any secondary peaks indicates good stoichiometry and phase purity of our sample.
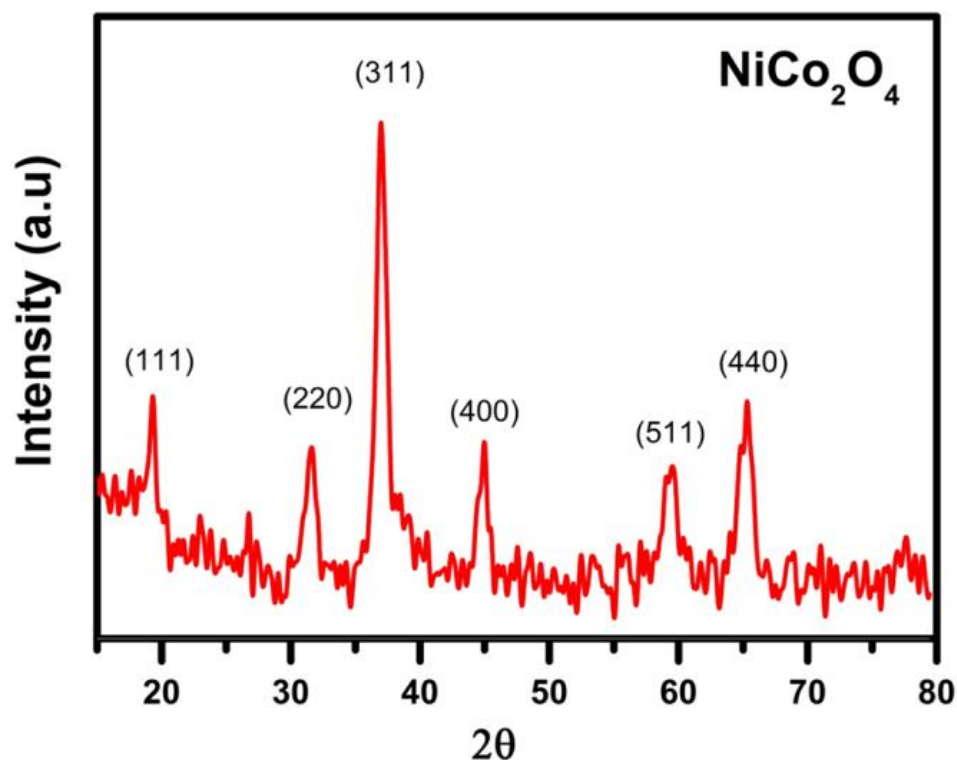
Figure 5: Powder X-ray diffraction pattern of $NiCo_2O_4$ nanowires.

Morphological features of $NiCo_2O_4$ nanowires were analyzed from SEM and TEM images. SEM images are shown in figure (6). We can clearly identify the presence of $NiCo_2O_4$ nanowires. These nanowires are assembled together to form a porous hierarchical network. The presence of the surfactant is responsible for the formation of this network. The surfactant helps the individual nanowires to assemble by Van der Waal forces and hydrogen bonding as reported for other surfactants for the synthesis of $NiCo_2O_4$ nanostructures[22]. As discussed later the specific network we obtain is particularly helpful for charge storage applications, since the ions can easily migrate into the inner part of the sample so that the overall electroactive area of the material is much more, resulting in enhanced pseudo-capacitive property and high rate cyclability.
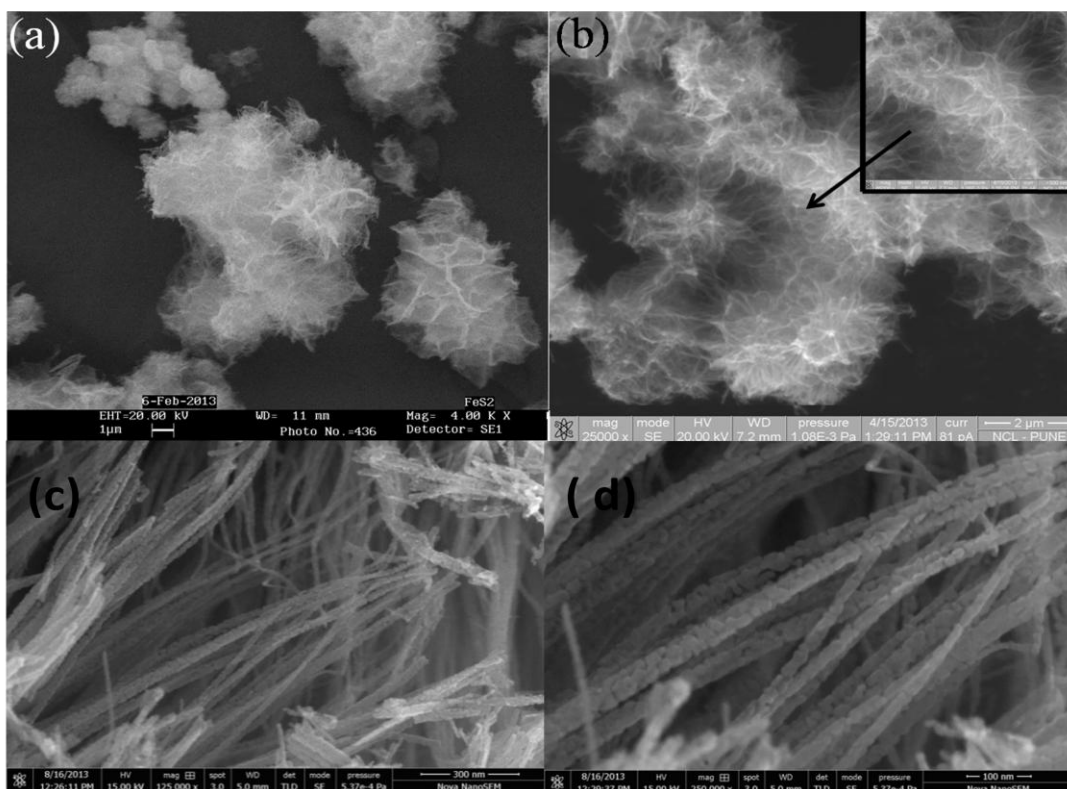
Figure 6: Scanning electron microscopy (SEM) images at low (a) and high (b) resolutions. The mean width of nanowires is around 60 nm

TEM images of $NiCo_2O_4$ are shown in figure (7) at three different magnifications. These images reveal the presence of nanowires with a width of around 60 nm. The TEM images show that the $NiCo_2O_4$ nanowires are polycrystalline and porous in nature. Every nanowire is comprised of tiny $NiCo_2O_4$ particles of size around 20 nm. Figure 7(b) depicts clustering of tiny $NiCo_2O_4$ particles into $NiCo_2O_4$ nanowires. High resolution TEM image of figure 7(c) shows lattice fringes with the d-spacing of 4.66 A$^\circ$ which corresponds to (111) plane of the $NiCo_2O_4$ crystal lattice. Selected area electron diffraction (SAED) pattern of figure 7(d) shows bright spots which imply that $NiCo_2O_4$ nanowires are highly crystalline in nature. Observed diffraction rings are indexed according to their miller indices.
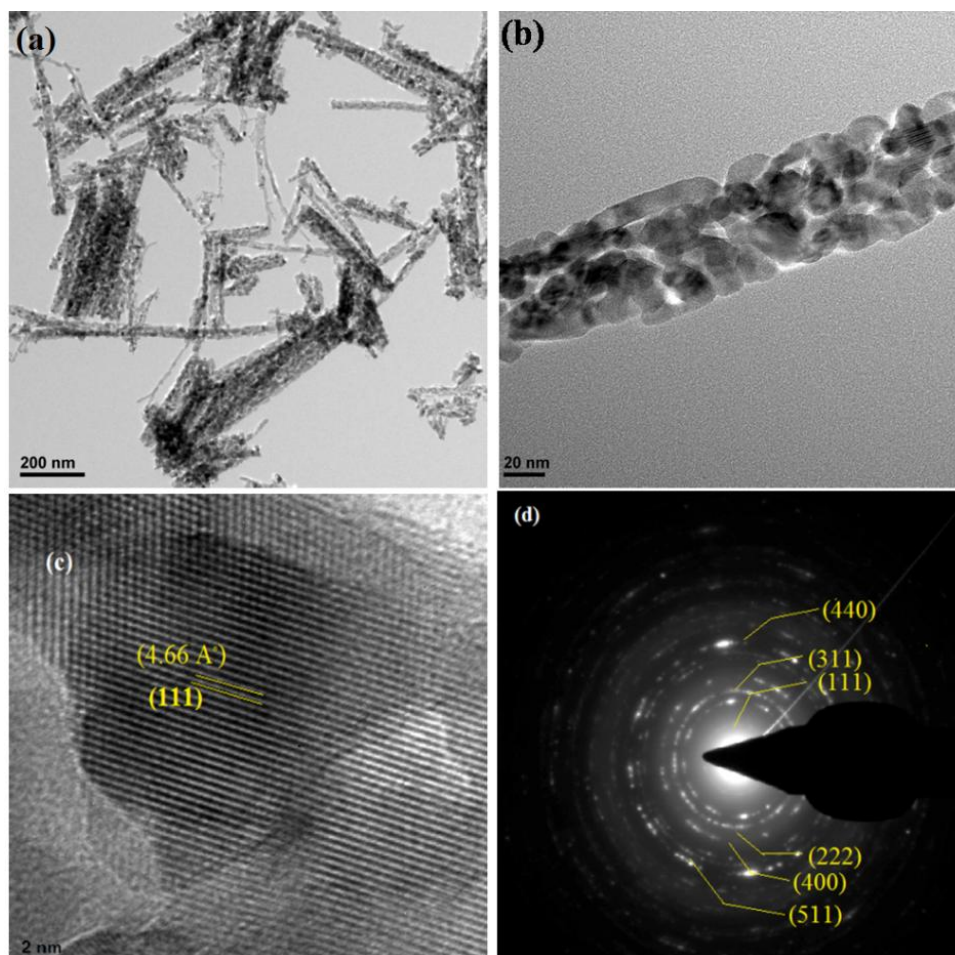
Figure 7: (a) and (b) Transmission electron microscopy (TEM) images NiCo$_2$O$_4$ nanowires, (c) HR-TEM image of NiCo$_2$O$_4$ nanowires, (d) selected area diffraction (SAD) pattern of NiCo$_2$O$_4$ nanowires with the observed diffraction rings indexed with corresponding miller indices.

From the above SEM and TEM images we can conclude that NiCo$_2$O$_4$ nanowire assembly is highly porous, and hence they possess high electroactive surface area which can facilitate higher electrochemical redox reaction rates, making this a suitable electrode material for supercapacitor applications.

Pore structure and specific surface area of NiCo$_2$O$_4$ nanowires was carried out using BET measurements. Figure (8 a) shows nitrogen adsorption/desorption isotherms. Surface area of the nanowires is 68.062m^2/g. The isotherm represents a hysteresis loop, a secondary process named capillary condensation is associated with loop. This process starts at about P/P$_O$ = 0.5 and ends at P/P$_0$ =1, which reveals complete filling of the mesopores and a high porosity of NiCo$_2$O$_4$ nanowires, which is also confirmed by TEM images. Figure 8(b) shows pore volume plot for NiCo$_2$O$_4$ nanowires, with a pore volume of 0.257 cc/g. Figure consists of three trimodal size

distribution at 4.5 nm, 5.7 nm and 13.3 nm, with maximum number of pores lying between 2nm – 5 nm which is an ideal size for materials with high electrochemical supercapacitor application.[33]
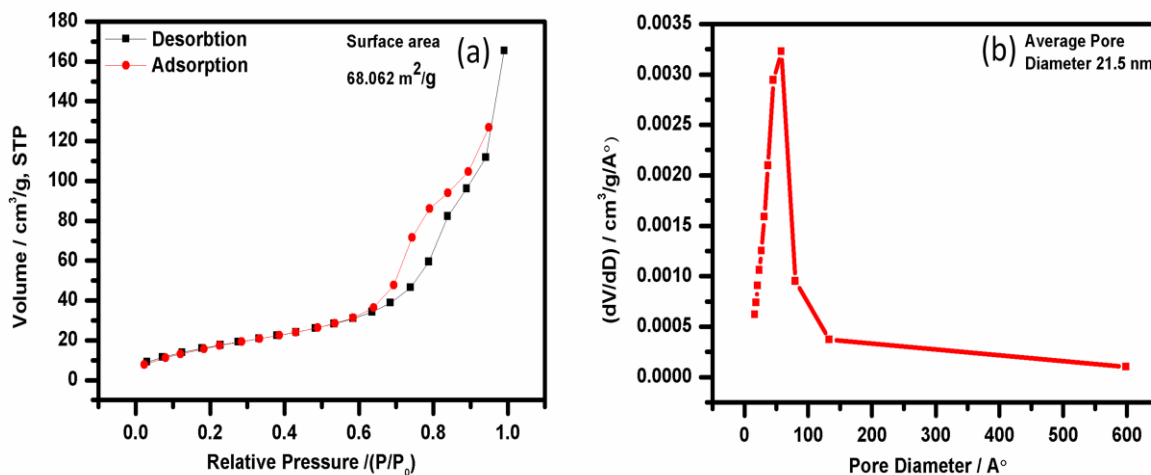
Figure 8: BET plots of NiCo$_2$O$_4$ nanowires (a) Nitrogen adsorption/desorption isotherms.
(b) Pore size distribution.

Electrochemical measurements like CV, charge discharge and impedance were therefore used to measure the electrochemical behavior of this electrode material. First, the CV plots were used to judge capacitive properties of the electrode material. Figure 9 (a) shows a typical CV curve for our NiCo$_2$O$_4$ material in the potential range -0.1 to 0.45V with various scan rates from 1 to 10 mV/s.
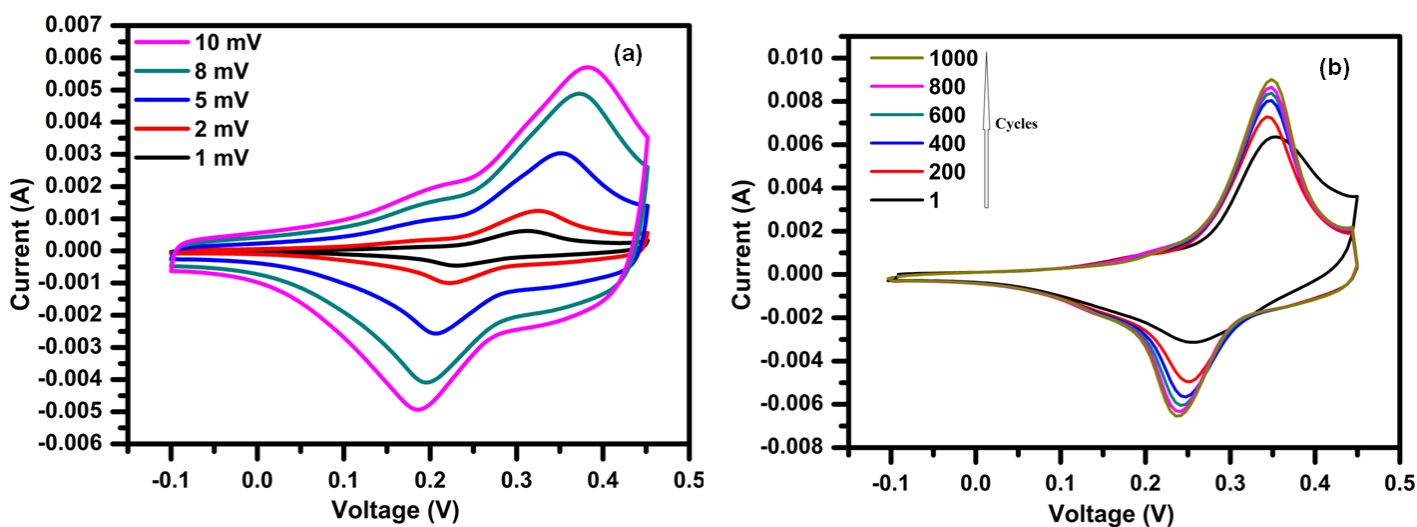
Figure 9: (a) Cyclic voltametry (CV) of NiCo$_2$O$_4$ electrode in 2M KOH, (b) the performance of NiCo$_2$O$_4$ electrode after every 200 cycles.

The CV of the electrode material was also performed up to 1000 cycles to check the stability of the nanowires at the scan rate of 10 mV/s. Figure 9(b) shows CV plots for every 200 cycles. It may be noted that as the number of cycles increases, there is no degradation of the current but rather an increment takes place. This increment indicates stronger redox reactions after successive cycling. This can be attributed to long cycling activation which generates far more available reactive sites in long-cycled electrodes than the fresh electrodes[33]. After 1000 cycling, 23% enhancement of the capacitance takes place (calculated from area under the curve) which confirms high stability of synthesized $NiCo_2O_4$ nanowires. These values can be easily compared with electrodes made with other NCO based supercapacitor electrode. [14, 15, 16, 34, 35]. Table (1) shows detailed comparision of the other NCO based supercapacitors.

In the cyclic voltametry a pair of strong redox peak is obtained which is far from the typical rectangular curve of the EDLC type supercapacitor. The strong redox peaks confirm the pseudocapacitive nature of the $NiCo_2O_4$ nanowire assembly, derived from the faradic reactions of the hydroxyl ions with metal ions present on the surface [33]. Electrochemical reactions occurring at NCO electrodes can be expressed as follows[29, 30].
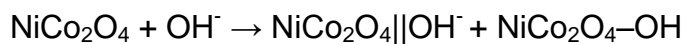
$$NiCo_2O_4 + OH^- \rightarrow NiCo_2O_4||OH^- + NiCo_2O_4–OH$$
$$NiO + XOH^- \rightarrow XNiOOH + (1-X)NiO + Xe^-$$

It is observed that with increasing scan rate the anodic peak current shifts towards the higher voltage and cathodic peak current shifts towards the lower voltage. This is because of the limitation of diffusion of ions at the higher scan rate which is common for all the powder based pseudocapacitive materials. Also it is important to notice that the oxidation and reduction reactions are highly reversible in nature which is important for the practical application.

High Rate of discharge and better cyclic performance of an electrode material are crucial for supercapacitor applications. Electrochemical behavior of $NiCo_2O_4$ nanowires was examined by charge-discharge method with three electrodes assembly at various current density values of 2, 4, 10, 20,40 A/g in the potential range from 0 to 0.45 mV and the results are shown in figure 8 (a). Discharge curves of the $NiCo_2O_4$ nanowires are clearly different from those for the double-layer capacitor which are linear in nature.[33] Nonlinearity of figure 10 (a) again represents

pseudo-capacitive behavior resulting from the electrochemical oxidation/reduction or redox reaction of the electrode material[1]. Values of specific capacitance were obtained by using following formula:

$$Cs = I/m \ (\Delta V/\Delta t)$$

Where I is the applied current density, m is the loading of $NiCo_2O_4$ material on the electrode, ΔV is the voltage window and Δt is the discharge time. The specific capacitance values are found to be 806.5, 840.58, 777.45, 628.15, and 508.3 F/g at specific current densities of 2, 4, 10, 20 and 40 A/g. These values of specific capacitance are higher than some previous reports for $NiCo_2O_4$ nanowires synthesized by different methods [15, 22].

Clearly, the porosity of the individual nanowires and the hierarchical network formation together increase the electro-active area, and thereby the overall charge storage property. Charge-discharge measurements were performed also at high current densities to check the high rate capability. At high current densities, the capacitance values are very important for high energy density supercapacitor application. In the case of NCO NWs assembled nanostructure, after cycling for 20 times at higher current density (40A/g), the capacitance was seen to reduce by 37% which is very good for high rate supercapacitor application. High rate capability confirms higher accessibility of the nanowires by the electrolytes even at high current density as well as high conductivity. High accessibility of the material is again because of easy diffusion of electrolytes into the porous network. Specific capacitance value at specific current density of 4A/g is highest (even greater than 2A/g) because most of the large parts of its reactive sites contribute to the specific capacitance value at this current density. This kind of behavior was also reported in the literature in the case of $NiCo_2O_4$ electrode material [6, 33].
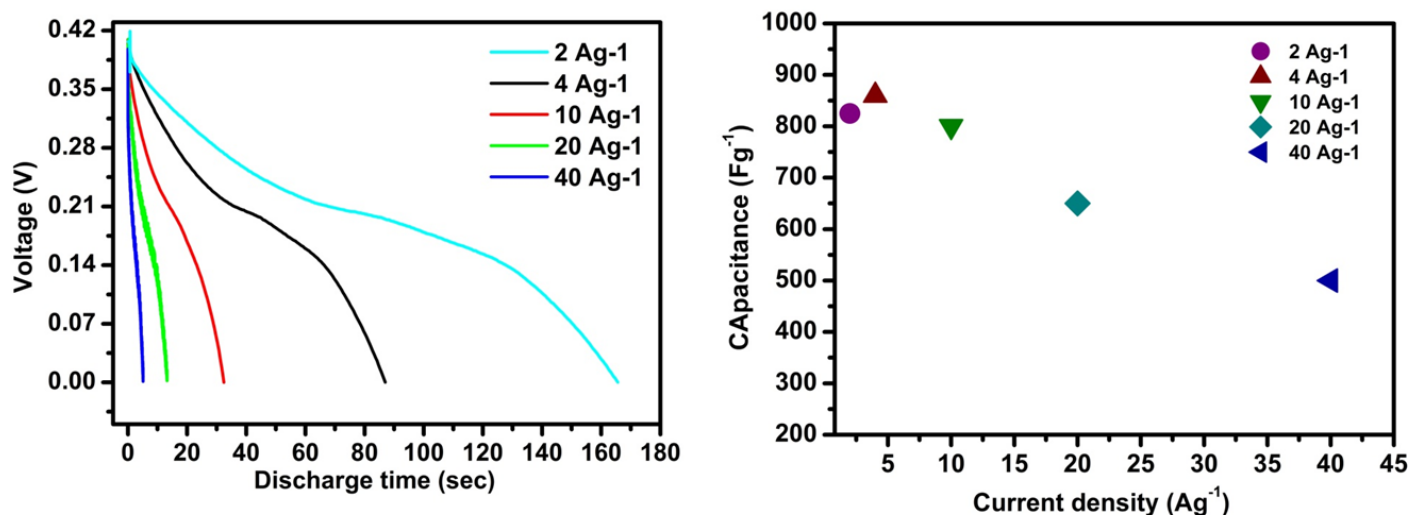
Figure 10: (a) Discharge time for NiCo$_2$O$_4$ electrode at different current densities, (b) Capacitance at different current densities, with maximum specific capacitance Of 840.58 F/g at 4 A/g.

Material	Specific Capacitance	Rate Capabilities	Cyclability
NiCo$_2$O$_4$ nanowires (present work)	806 F g^{-1} @ 2 A g^{-1}	63 % (1 to 40 A g^{-1})	123% (1000 cycles)
NiCo$_2$O$_4$ Nanosheets (ref 34)	560 F g^{-1} @ 1 A g^{-1}	40 % (4 to 10 A g^{-1})	94 % (2000 cycles)
Porous NiCo$_2$O$_4$ Nanowires (ref 22)	743 F g^{-1} @ 1 A g^{-1}	78.6 % (1 to 40 A g^{-1})	93.8% (2000 cycles)
Urchin-like NiCo$_2$O$_4$ (ref 14)	658 F g^{-1} @ 1 A g^{-1}	81 % (1 to 10 A g^{-1})	98% (1000 cycles)
NiCo$_2$O$_4$ Nanoparticles (ref 16)	659 F g^{-1} @ 1 A g^{-1}	53 % (1 to 16 A g^{-1})	48% (300 cycles)
NiCo$_2$O$_4$ nanowires (ref 15)	760 F g^{-1} @ 1 A g^{-1}	70 % (1 to 20 A g^{-1})	81% (3000 cycles)
NiCo$_2$O$_4$ film (ref 35)	570 F g^{-1} @ 1 A g^{-1}	100 % (1 to 50 A g^{-1})	94% (2000 cycles)
NiCo$_2$O$_4$ Nanosheets on carbon nanofibres (ref 36)	1002 F g^{-1} @ 1 A g^{-1}	67.3 % (1 to 10 A g^{-1})	92.75% (2400 cycles)
NiCo$_2$O$_4$ Crystals (ref 37)	216 F g^{-1} @ 1 mA cm^{-2}	87 % (1 to 20 mA cm^{-2})	96% (600 cycles)

Table 1: Detailed comparision of other NCO based supercapacitors

Electronic resistance is an important parameter to know about the capacitance of the material; lower electronic resistance (or higher electronic conductivity) implies higher capacitance and higher power density of the material. AC impedance technique (Electrochemical impedance Spectroscopy measurement) was therefore used as a tool to measure the electronic resistance of NiCo$_2$O$_4$. Figure (11) shows the complex

plane impedance plot (imaginary part, Z" Versus real part, Z') for $NiCo_2O_4$ electrode between 0.1 Hz to 10^5 Hz, to measure the intrinsic resistance and relative capacitive performance. The impedance plot, both at higher and lower frequency, was analyzed. Difference in conductivity between the solid oxide (electronic conductivity) and the liquid electrolyte phase (ionic conductivity) leads to discontinuity in the charge transfer between the solid oxide and electrolyte interface, and hence the Nyquist plot shows semicircular nature at larger frequency. Linear line at lower frequency indicates Warburg impedance, W, which arises due to resistance for OH^- ions in the electrode material. Since the diffusion of OH^- ions is not the same in the liquid electrolyte and solid electrode material, due to differences in the diffusive resistance of electrolyte in electrode pores and ion diffusion in the host material, finite slope appears as shown in figure 10. EIS plot in fig.6 shows the equivalent series resistance (ESR) of 5.7Ω with Warburg line at 45^0 to the Z' axis showing the enhanced diffusion of electrolyte ions inside the electrode material, thus reflecting the highly porous nature of NCO NW assembled electrode as is also confirmed by the SEM images.
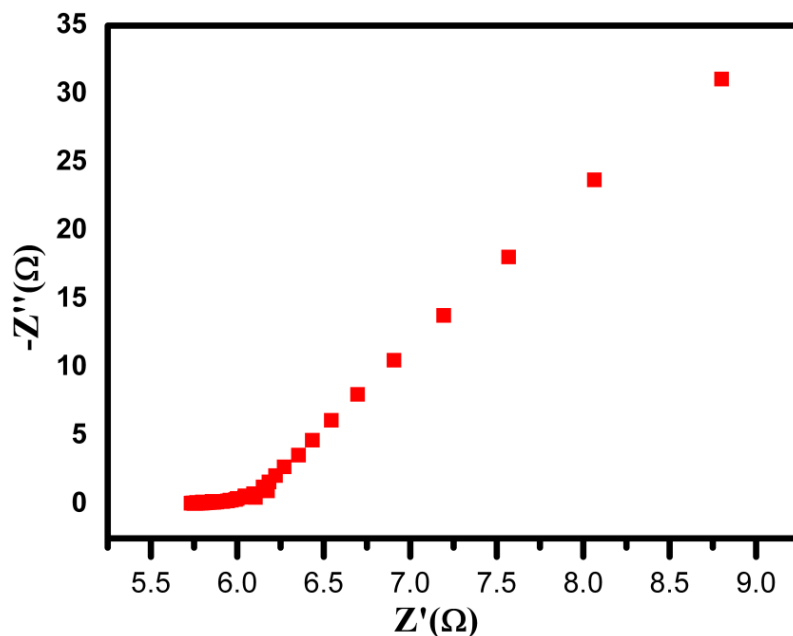
Figure 11: Complex plane impedance plots (Nyquist plot) for the $NiCo_2O_4$ electrode

1.4 Conclusion

In conclusion, we demonstrate facile synthesis of $NiCo_2O_4$ nanowires with a unique porous morphology by calcination of hydrothermally synthesized nickel cobalt hydroxide carbonate. The electrode coated with this material shows very high specific capacitance of 840 F/g at a current density of 2 A/g. Also this NCO NWs nanostructure exhibits high rate capability (63% retention of capacity after cycling current density from 2 to 40 A/g) and good cyclibility (100% retention and 23% enhancement of capacitance after cycling 1000 cycles). Such fascinating capacitive performance of $NiCo_2O_4$ is attributed to its high surface area and the specific nature of porosity. Synthesis of $NiCo_2O_4$ nanowires in the powered form renders a key advantage that we can choose and change the degree of loading of the electrode material and increase the volumetric capacitance of the supercapacitor by loading higher amount of electrode material in smaller area.

2. Nanoporus NiCo$_2$O$_4$ sheet for enhanced Supercapacitor Application

For an electrode material to be effectively used for supercapacitor application, the geometry and morphology of the synthesized material must be such that its whole surface is utilized and it must have appropriate pore size for fast ion transport through it which results in rapid faradic mechanism. Higher surface area, pore size, geometry, and crystallinity of the electrode material effects electrochemical performance of the pseudo-capacitor. Electrode material must be engineered to produce a unique geometry and morphology, which generates higher surface area, optimized pore size and higher electrical conductivity which facilitates in increasing the power and energy density of the pseudo-capacitors [38]. It has been reported in previous reports that materials having long range (micrometer in length) and thin (nanometer in thickness) gives an enhanced performance for electrochemical supercapacitor application.[39] Long range morphology lowers the internal resistance of the materials hence accelerating the electron transport rate for fast faradic reactions compared to nanostructures composed of noncontinuous nanoparticles[40] ,thin thickness facilitate short ion diffusion path and larger surface area which greatly increases the capacitance. Growth of a 2D nanoporous sheet like structure is an ideal morphology for enhanced supercapacitor performance. Its long range order and thin thickness makes it an effective material in energy storage devices.

I report a different morphology of NiCo$_2$O$_4$. I obtained mesoporous network of interconnected NiCo$_2$O$_4$ nanosheets, as explained above this nanostructure enables faster redox reactions and delivers a high specific capacitance of 1763.19 Fg^{-1} at a current density of 1 Ag^{-1} and it decreased by 32.69 % by decreasing current density from 1 Ag^{-1} to 40 Ag^{-1}. As I have mentioned in my earlier work that most of the reported NiCo$_2$O$_4$ morphologies have been synthesized on some substrates, in this work also, I synthesized NiCo$_2$O$_4$ in powdered which increase the loading on the electrode in a smaller area, which increases its volumetric capacitance. We obtained NiCo$_2$O$_4$ in a bulk amount by hydrothermal synthesis, which makes it a commercially important product. Due to its unique morphology NiCo$_2$O$_4$ nanosheets shows a high specific capacitance of 1763.19 Fg^{-1} which is high comparable with other previously reported for NiCo$_2$O$_4$ morphologies.

2.1 Experimental Section

Nickel nitrate hexahydrate $(Ni(NO_3)_2).6H_2O$, cobalt nitrate hexahydrate $(Co(NO_3)_2).6H_2O$, ammonia (NH_3) were purchased from merck. Hexamethylenetetramine (HMTA) was purchased from sigma Aldrich. All chemicals were of analytical grade and were used without any further purification. In a typical procedure 3 mmol of $Ni(NO_3)_2.6H_2O$, 6mmol of $Co(NO_3)_2.6H_2O$ and 6 mmol of HTMA were mixed uniformly in a solution of 50 ml of water and 30 ml of ethanol and stirred for 15 mintues. After that 2 ml of NH_3 is added to this mixture. The mixture was subsequently stirred. The solution was then transferred to Teflon lined stainless steel autoclave of 100 ml capacity and was subjected to heating at $90°C$ for 6 h. After cooling the autoclave to room temperature, a light green solid precipitate was observed which was separated by centrifugation at 10000 rpm with successive repeated washings with water, ethanol-water and pure ethanol. The precipitate was dried at $60°C$ in vacuum, and then annealed at $300°C$ at a heating rate of $1°C/min$ for 24 hours. After cooling it down to room temperature, black-colored $NiCo_2O_4$ powder was obtained which was subjected to further characterizations and electrochemical measurements.

2.2 Characterization

Powder X-ray diffraction (XRD) pattern was recorded using Philips X'Pert PRO by Cu K_α radiation. Electron microscopy was performed with FE-SEM (Hitachi S-4200) and HR-TEM (HR-TEM, FEI Tecnai 300). All the electrochemical measurements were conducted in three electrode assembly. The composite electrode was made up by slurry of appropriate amount of active material $(NiCo_2O_4)$, conductive additive (Super P), binder (Polyvinylidene fluoride) and 1-methyl-2-pyrrolidinone (NMP) with ratio of 8:1.5:0.5. The slurry was then coated on one side of graphite electrode and dried at $60°C$ for 12 hours. The graphite electrode coated with slurry of $NiCo_2O_4$ served as working electrode, while a platinum strip and Ag/AgCl (saturated KCL) served as counter and reference electrodes, respectively. All the experiments were carried out using freshly prepared 2M KOH solution. The electrochemical impedance measurement was performed between 0.1 and 10^5 Hz with the voltage amplitude of 5mV.

2.3 Results and discussion:

Uncalcined nickel cobalt hydroxide was first synthesized in a teflon-lined stainless steel autoclave at 90°C for 6 hours with a solution of $Ni(NO_3)_2.6H_2O$, $Co(NO_3)_2.6H_2O$,HMTA in water and ethanol. By simply replacing urea with HMTA, we get 2D uniform nanostructured $NiCo_2O_4$ ultrathin nanosheets. HMTA functions in coordinating itch of nickel cobalt hydroxide, releasing OH^{-1} to facilitate recrystallization of nickel cobalt hydroxide carbonate. Experimental parameters which influence the hydrolysis rate and control the nucleation as well as crystal growth processes, such as concentration of metal salt solution, HMTA, reaction temperature and time were carefully optimized for the reproducible formation of $NiCo_2O_4$ nanosheet with the desired morphology and properties.

Figure (12) shows a characteristic powder x-ray diffraction (PXRD) pattern of $NiCo_2O_4$ with d-values 2.85A°, 2.017A°, 1.55A°, 1.42A°, assigned to the planes (311), (400), (511), (440), respectively, of the nanostructured cubic type $NiCo_2O_4$. Absence of any secondary peaks indicates good stoichiometry and phase purity of our sample.
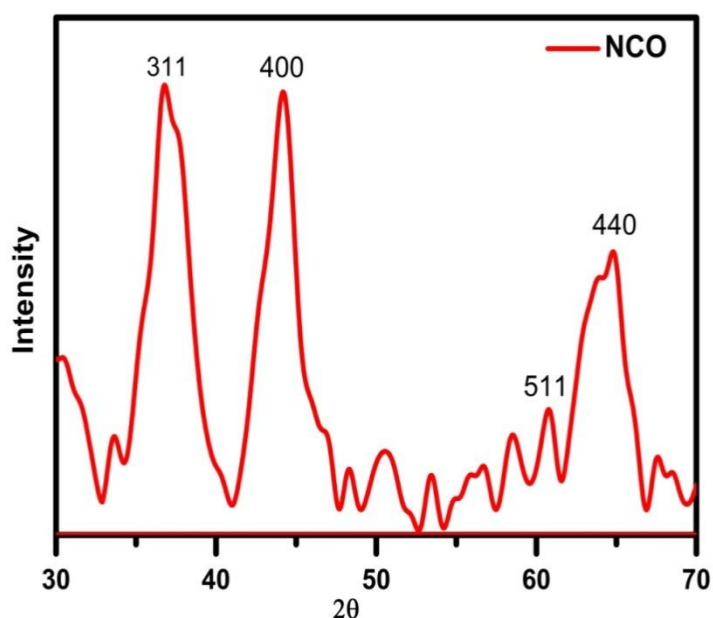

Figure 12: Powder X-ray diffraction pattern of NiCo$_2$O$_4$ nanosheet

Morphological features of NiCo$_2$O$_4$ nanosheet were analyzed from SEM and TEM images. SEM images are shown in figure (13). Formation of NiCo$_2$O$_4$ nanosheets can be easily visualized with these images. Figure (13 a) shows hierarchical architecture of 2D NiCo$_2$O$_4$ nanostructure. It can be seen that the nanostructure is composed of uniformly interconnected ultrathin nanosheets. Nanostructures of NiCo$_2$O$_4$ assembled together to bring forth uniformly dispersed NiCo$_2$O$_4$ nanosheet. Figure (14) shows the TEM images at various magnifications. Unique flower like morphology can be easily seen at lower magnification figure (14 a). NiCo$_2$O$_4$ nanosheets are very thin and highly porous, scattered uniformly, which reveals its high surface area. The mesoporous feature of the NiCo$_2$O$_4$ nanosheets largely increases the amount of electroactive sites, which facilitates transport of the ions, making it a highly suitable material for supercapacitor. High resolution TEM image of figure (14 c) shows lattice fringes with the d-spacing of 2.7 A$^\circ$ which corresponds to (311) plane of the NiCo$_2$O$_4$ crystal lattice

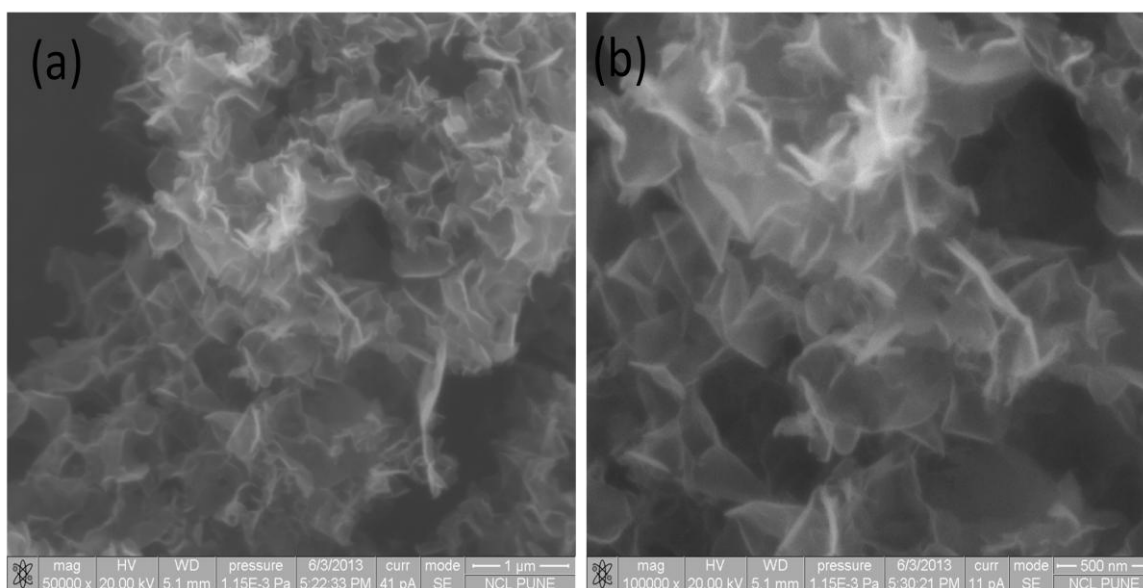**Figure 13: Scanning electron microscopy (SEM) images of NiCo$_2$O$_4$ nanosheet (a) At lower magnigication (1 μm). (b) At higher magnification (500 nm).**
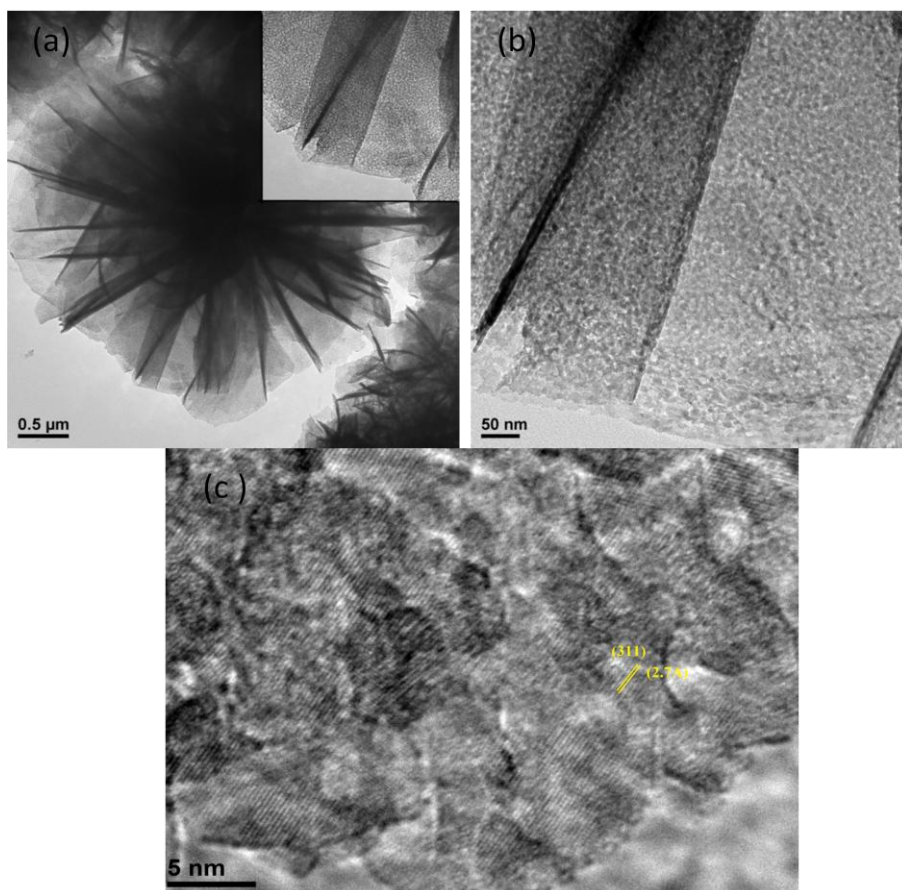
Figure 14: (a) and (b) Transmission electron microscopy (TEM) images NiCo$_2$O$_4$ nanosheet, (c) HR-TEM image of NiCo$_2$O$_4$ nanowires.

From the above SEM and TEM images we can conclude that NiCo$_2$O$_4$ nanosheet assembly is highly porous, and hence they possess high electroactive surface area which can facilitate higher electrochemical redox reaction rates, making this a suitable electrode material for supercapacitor applications.

Electrochemical measurements like CV, charge discharge and impedance were therefore used to measure the electrochemical behavior of this electrode material.

First, the CV plots were used to judge capacitive properties of the electrode material. Figure (15 a) shows a typical CV curve for our NiCo$_2$O$_4$ material in the potential range -0.1 to 0.45V with various scan rates from 2 to 50 mV/s. In the cyclic voltametry a pair of strong redox peak is obtained which is far from the typical rectangular curve of the EDLC type supercapacitor. The strong redox peaks confirm the pseudocapacitive nature of the NiCo$_2$O$_4$ nanosheet assembly, derived from the faradic reactions of the hydroxyl ions with metal ions present on the surface.

It is observed that with increasing scan rate the anodic peak current shifts towards the higher voltage and cathodic peak current shifts towards the lower voltage. This is because of the limitation of diffusion of ions at the higher scan rate which is common for all the powder based pseudocapacitive materials. Also it is important to notice that the oxidation and reduction reactions are highly reversible in nature which is important for the practical application.
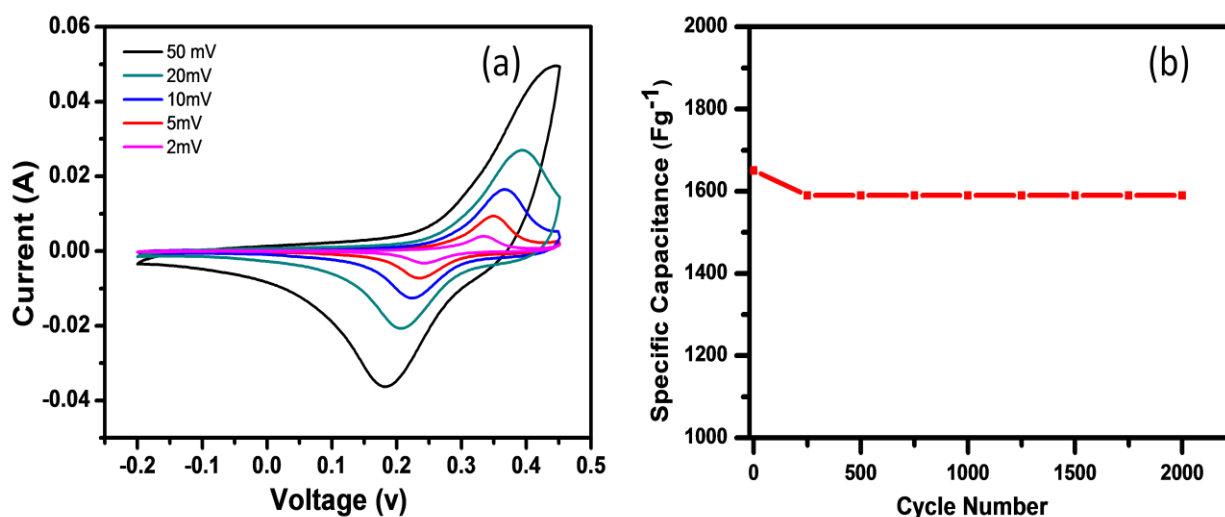
Figure 15: (a) Showing cyclic voltametry (CV) of NiCo$_2$O$_4$ nanosheet. (b) Showing stability data of NiCo$_2$O$_4$ nanosheet.

Figure (15 b) shows stability plot for NiCo$_2$O$_4$ nanosheet up to 2000 cycles. NiCo$_2$O$_4$ shows exceptionally high stability with only 3.68 % decrease in specific capacitance value at 5 mV/s.

High Rate of discharge and better cyclic performance of an electrode material are crucial for supercapacitor applications. Electrochemical behavior of NiCo$_2$O$_4$ nanosheet was examined by charge-discharge method with three electrodes assembly at various current density values of 1, 2, 3, 5,10,20, 40 A/g in the potential range from 0 to 0.45 mV and the results are shown in figure (16 a). Discharge curves of the NiCo$_2$O$_4$ nanosheet are clearly different from those for the double-layer capacitor which are linear in nature. Nonlinearity of figure (16 a) again represents pseudo-capacitive behavior resulting from the electrochemical oxidation/reduction or redox reaction of the electrode material. Values of specific capacitance were obtained by using following formula:

$$Cs = I/m \ (\Delta V/\Delta t)$$

Where I is the applied current density, m is the loading of $NiCo_2O_4$ material on the electrode, ΔV is the voltage window and Δt is the discharge time. Table 2 shows specific capacitance obtained at different current density.
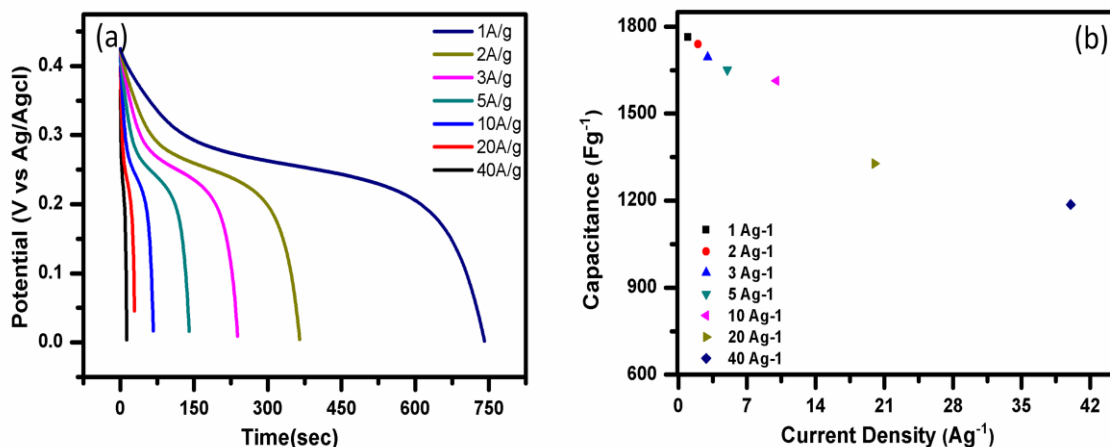
Figure 16 (a) Discharge time for NiCo₂O₄ electrode at different current densities, (b) Capacitance at different current densities, with maximum specific capacitance of 1763.19 F/g at 1 A/g.

Specific Capacitance (F g-1)	Current density (A g-1)
1763.19	1
1738.69	2
1694.46	3
1650.83	5
1613.33	10
1327.62	20
1186.67	40

Table 2: Specific capacitance value for NiCo₂O₄ at different current density.

Clearly, the porosity of the nanosheet and the hierarchical network formation together increase the electro-active area, and thereby the overall charge storage property. Charge-discharge measurements were performed also at high current

densities to check the high rate capability. At high current densities, the capacitance values are very important for high energy density supercapacitor application. In the case of NCO nanosheets assembled nanostructure, after cycling at 40 time's higher current density (40A/g), the capacitance was seen to reduce by 32.69% which is very good for high rate supercapacitor application. High rate capability confirms higher accessibility of the nanosheets by the electrolytes even at high current density as well as high conductivity. High accessibility of the material is again because of easy diffusion of electrolytes into the porous network.

Electronic resistance is an important parameter to know about the capacitance of the material; lower electronic resistance (or higher electronic conductivity) implies higher capacitance and higher power density of the material. AC impedance technique (Electrochemical impedance Spectroscopy measurement) was therefore used as a tool to measure the electronic resistance of $NiCo_2O_4$. Figure (18) shows the complex plane impedance plot (imaginary part, Z" Versus real part, Z') for $NiCo_2O_4$ electrode between 0.1 Hz to 10^5 Hz, to measure the intrinsic resistance and relative capacitive performance. The impedance plot, both at higher and lower frequency, was analyzed. Difference in conductivity between the solid oxide (electronic conductivity) and the liquid electrolyte phase (ionic conductivity) leads to discontinuity in the charge transfer between the solid oxide and electrolyte interface, and hence the Nyquist plot shows semicircular nature at larger frequency. Linear line at lower frequency indicates Warburg impedance, W, which arises due to resistance for OH^- ions in the electrode material. Since the diffusion of OH^- ions is not the same in the liquid electrolyte and solid electrode material, due to differences in the diffusive resistance of electrolyte in electrode pores and ion diffusion in the host material, finite slope appears as shown in figure (18). EIS plot in fig.6 shows the equivalent series resistance (ESR) of 0.9Ω with Warburg line at 45^0 to the Z' axis showing the enhanced diffusion of electrolyte ions inside the electrode material, thus reflecting the highly porous nature of NCO nanosheet assembled electrode as is also confirmed by the TEM images.

.
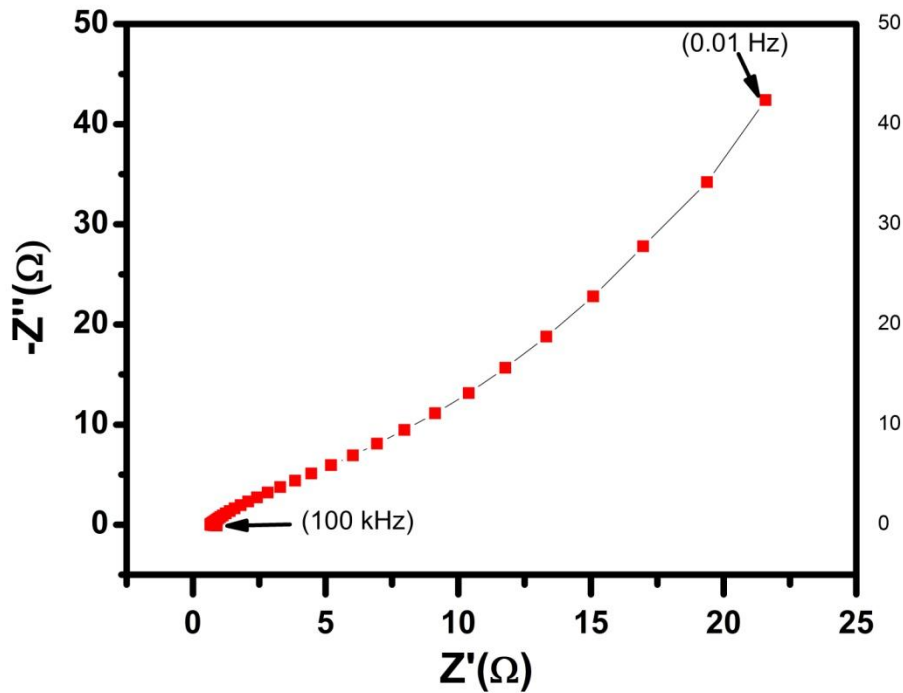
Figure 17: Complex plane impedance plots (Nyquist plot) for the NiCo$_2$O$_4$ electrode

2.4 Conclusion

In summary I synthesized Nickel cobalt oxide nanosheets, and coated on graphite to analyze its electrochemical performance for supercapacitor application. Comparing from my earlier report on Nickel oxide nanowires, these nanosheets gave an higher capacitance value, because of changing its morphological feature, by changing 1D nanowires to 2D nanosheets. Nanosheet having long range and thin thickness gives them advantage of lower internal resistance which accelerates the faradic reactions by increasing electron transport rate through the material and also such feature has a higher ion adsorption/extrusion rates and larger surface area, making its capacitance large in comparison to 1D nanostructures, in my case Nanowires. NCO nanosheet gave a high capacitance of 1763.19 F/g at a current density of 1 A/g and showed an excellent stability with only 3% decrement in capacitance value. Synthesis of NCO nanosheet in powdered form makes it a commercially useful product.

3. Nickel foam supported nickel cobalt sulfide 3D ultrathin porous nanosheet
For high rate performance supercapacitor

Of all the binary transition metal oxides and sulfides, nickel and cobalt oxides/sulfides have been found to be the materials of choice with regard to their non-toxicity, low cost, and various suitable nanostructures for high specific capacitance values[41-45] Bur very recently extensive work on the synthesis of pure phase ternary oxide nanostructures is currently in progress for good performance in charge storage applications[46,47] Nickel cobalt sulfide (NCS) is one such structurally tunable, electrochemically active high conductive ternary sulfide. NCS possesses low band gap and better conductivity compared with corresponding oxide NCO and exhibited better rich electrochemistry due to synergy effect of two different atoms than the corresponding binary sulfides. It was already known that the conductivity of the NCS is greater than its corresponding oxide NCO and definitely better than cobalt and nickel oxide. A range of nanostructures including one-dimensional nanowire have been reported for NCS as an electrode material in supercapacitors. For example, Ruan and coworkers reported porous nanotube of NCS with maximum specific capacitance 1093 Fg^{-1} at a current density of 0.2 Ag^{-1} and Xia et al. reported the specific capacitance of 1149 at the current density of 1 Ag^{-1}. Despite several reports on ternary NCS were directly grown on various conductive substrate for improve the capacitance performance. Very recently Wang et al[48] synthesized ternary NCS nanotube on nickel foam and demonstrated its efficient capacitive performance with 738 F g^{-1} at 4 A g^{-1} and Wang and co worker have grown single crystalline hollow nanotube of NCS with capacitance of 0.87 F cm^{-2} at

4 mA cm^{-2}.But unfortunately the rate performance is still not satisfactory. So there are still challenges to synthesize the novel nanostructure to improve the capacitance as well as the rate capability of NCS.

Morphology of the nanostructure is one of the most important desirable parameters for high performance pseudocapacitive electrode. In this respect high surface area porous nanostructure is expected to be crucial. High surface area nanostructure provides more electroactive surface area for enhancing the performance of the supercapacitor by adsorbing the ions via EDLC as well as faradic reaction. The adsorbed ions also act as a buffer layers for the fast reversible faradic reaction to happen during charging and discharging. Suitable porosity is equally important

because it helps faster ion transport into the bulk of the electrode to utilize the maximum electroactive surfaces of the material. Various nanostructures including nanowire, nanorod, hollow nanostructure, nanosheet have been reported for enhance the pseudocapacitive performance. Among them, the long range porous nanosheet with ultrathin thickness is regarded as the most promising candidates for high performance pseudocapacitor. Ultrathin thickness helps the maximum utilization of the atomic surfaces, long range helps inhibit electron hoping i.e. lower electron transport resistance and porosity helps for adsorption of ions via EDLC as well as faster ion transport. The combined effect helps to improve the capacitance performance of the material. But making film of the powder sample with insulating binder increases the resistance, cost and weight factors which are counter-productive to the capacitive performance. Also such film blocks very large portion of the electroactive surfaces of the electrode and thereby decreases the overall gravimetric capacitance of the material. Therefore, it is indeed very useful to directly grow desire nanostructures on a conductive substrate in order to generate an electrode for effective charge storage without the use of binders/additives.

By considering the above facts, in this work we report the one step synthesis of ultrathin NCS nanosheets by simple electro deposition method. The 2D porous ultrathin nanosheets were growth on the electrochemically robust nickel foam substrate to form the 3D hierarchical porous nanostructure. We have checked the electrochemical performance of as synthesized electrode in 3M KOH medium where it exhibited not only the ultrahigh capacitance, also very high rate performance and superior cyclability which fulfill all the criteria to be a promising electrode for supercapacitor.

3.2 Experimental Section:

3.2.1 Materials:

All the chemicals nickel chloride hexahydrate ($NiCl_2.6H_2O$), cobalt chloride hexahydrate ($CoCl_2.6H_2O$) and thiourea (CH_4N_2S) used for synthesis were analytical grade and commercially available from Merck Pvt. Ltd. and were used as received without further purification.

3.2.2 Electrode Preparation:

Cathodic deposition of NCS electroactive material was conducted in a deposition bath consisting of 20 mg of $NiCl_2.6H_2O$, 40 mg of $CoCl_2.6H_2O$ and 2.86 g thiourea .The PH of the solution is maintained to be around 6 by adding appropriate amount of NH_4OH. A three compartmental cell is used to carry out potentiodynamic deposition, with Ag/AgCl electrode acting as reference, platinum is used as counter electrode and substrate Ni foam is used as a working electrode. Potential range was set to be between -1.2 V to 0.2 V vs AgCl at a scan rate of 5 mV/s. Electrodeposition was carried out for 30 cycles followed by cleaning the substrate with DI H_2O and heating it in vacuum for 12 hrs at $80°C$.

3.2.3 Characterization and Measurement

Electron microscopy was performed with FE-SEM (Hitachi S-4200) and HR-TEM (HR-TEM, FEI Tecnai 300). All the electrochemical measurements were conducted in three electrode assembly. The Ni foam coated with NCS served as working electrode, while a platinum strip and Ag/AgCl (saturated KCL) served as counter and reference electrodes, respectively. All the experiments were carried out using freshly prepared 3M KOH solution. Electrochemical performance of the electrode was carried out by cyclic voltammeter (CV) and galvanostatic charge discharge.

3.3 Results and Discussion

3.3.1 To investigate the morphological features of the NCS nanosheet, its TEM was studied. Folded morphology with diaphanous nature of the nanosheets indicates its ultrathin nature as can be seen from the figure (19 b). High porosity of the material can be revealed from figure (19 c). Long ranged with thin thickness makes the nanosheets being puckered and crumpled. These unique morphological features greatly increases the surface area of the electrode material, which greatly increases charge storage properties, being ultrathin these nanosheets accelerates the rate of ion transport through them.
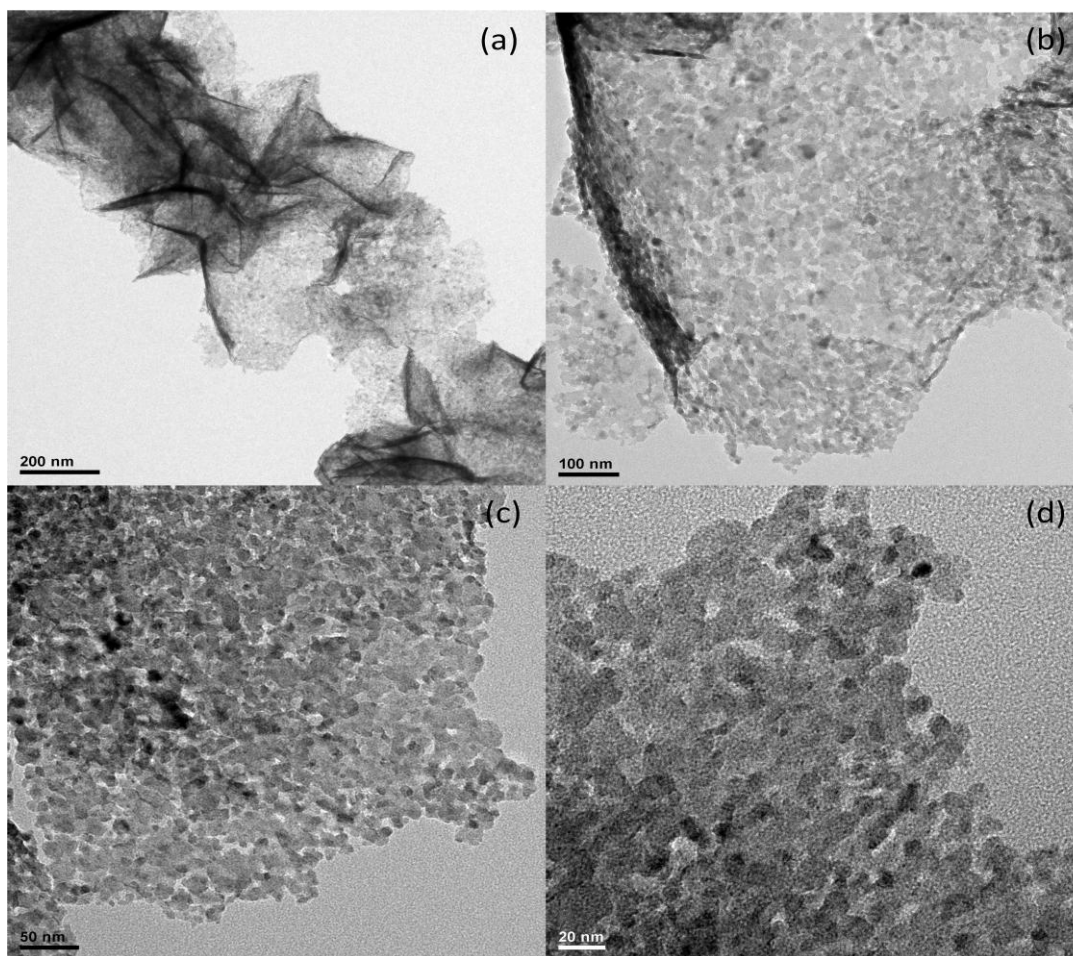
Figure 18: TEM images of NCS nanosheet at (a) 200 nm, (b) 100 nm
(c) 50 nm, and (d) 20 nm

3.3.2 Cyclic Voltammetry

The electrochemical measurement of NCS nanosheet was analysed by using cyclic voltammetry, in a potential range of 0 to 0.55 V vs Ag/AgCl at scan rates from 3 mV/s to 50 mV/s in a 3M KOH solution. Figure (20 a) shows current-voltage relationship at various scan rates. Symmetrical increase of peak current density at higher scan rates can be dictated from the figure. Therefore a linear relationship between anodic current density and scan rate can be seen in figure (20 b) Appearance of both oxidation and reduction peaks clearly indicate pseducapacitive nature of the NCS nanosheet and make it differ by EDLC which has a nearly rectangular nature. Figure (20 c) shows comparison of the CV curves at scan rate of 10 mV/s between bare Ni foam and Ni foam with NCS material, disappearance of redox peaks and a much lower current density in case of Ni foam clearly indicates

negligible contribution of the Ni foam in electrochemical capacitance. These results demonstrate excellent reversibility and high rate capability for NCS electrode, which can be attributed to the high surface area of the interlocked NCS nanosheet morphology and faster ion-diffusion rate within the electrode.
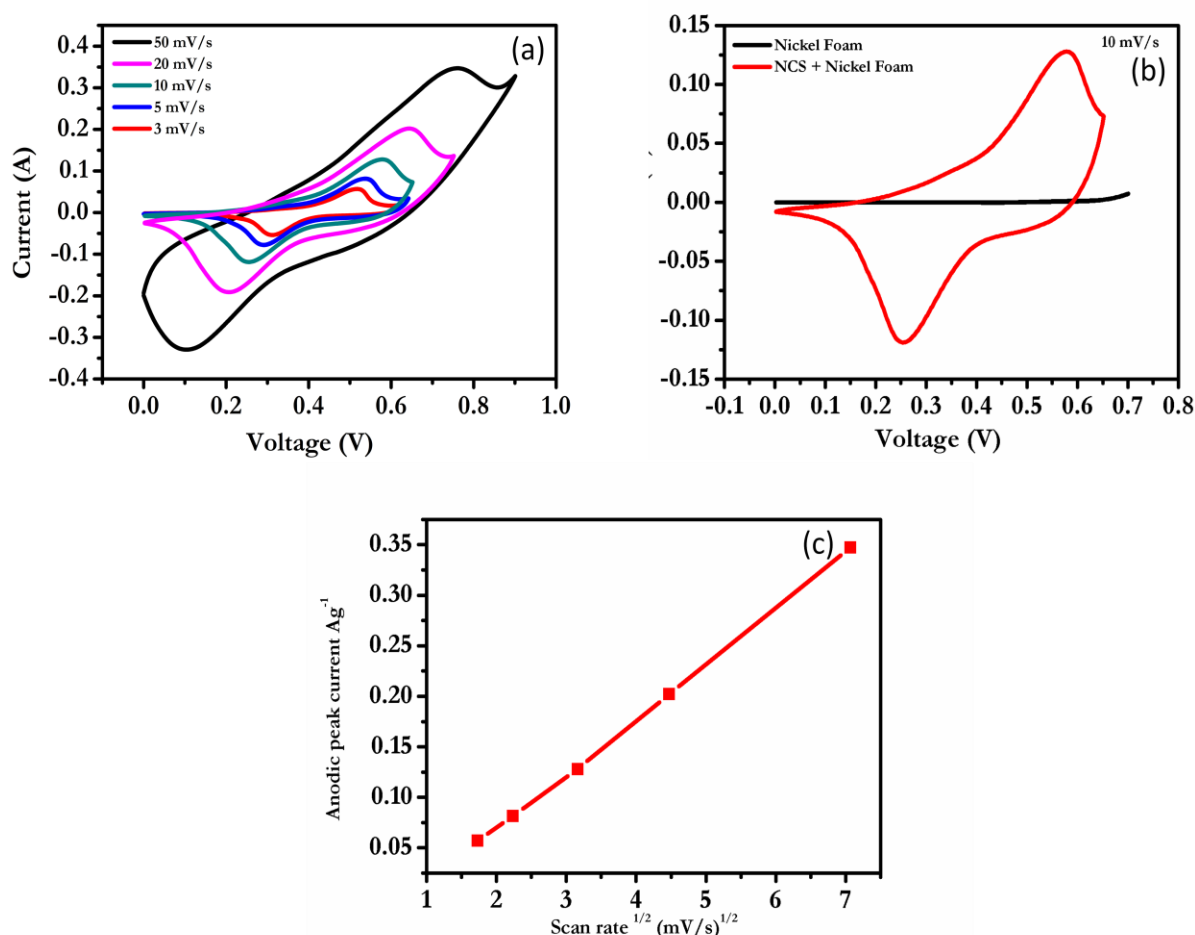
Figure 19: (a) Cyclic voltammetry curves for NCS nanosheet. (b) Comparison of the current density for Ni foam and Ni foam + NCS. (c) Linear relationship between anodic peak current and root of scan rate.

3.3.3 Galvanostatic Charge Discharge analysis

High Rate of discharge and better cyclic performance of an electrode material are crucial for supercapacitor applications. Electrochemical behavior of NCS nanosheet was examined by charge-discharge method with three electrodes assembly at various current density values of 1, 4, 8, 10, 15, 20, 30, 40, 50 A/g in the potential range from 0 to 0.55 mV and the results are shown in figure (21 a). Discharge curves of the NCS nanosheet are clearly different from those for the double-layer capacitor

which are linear in nature [33] Nonlinearity of figure (21 a) again represents pseudo-capacitive behavior resulting from the electrochemical oxidation/reduction or redox reaction of the electrode material [1].

Figure 20: (a) Discharge time for NCS nanosheet at different current density. (b) Specific capacitance at different current density, with maximum capacitance of 2186.36 Fg-1 at 1 Ag-1
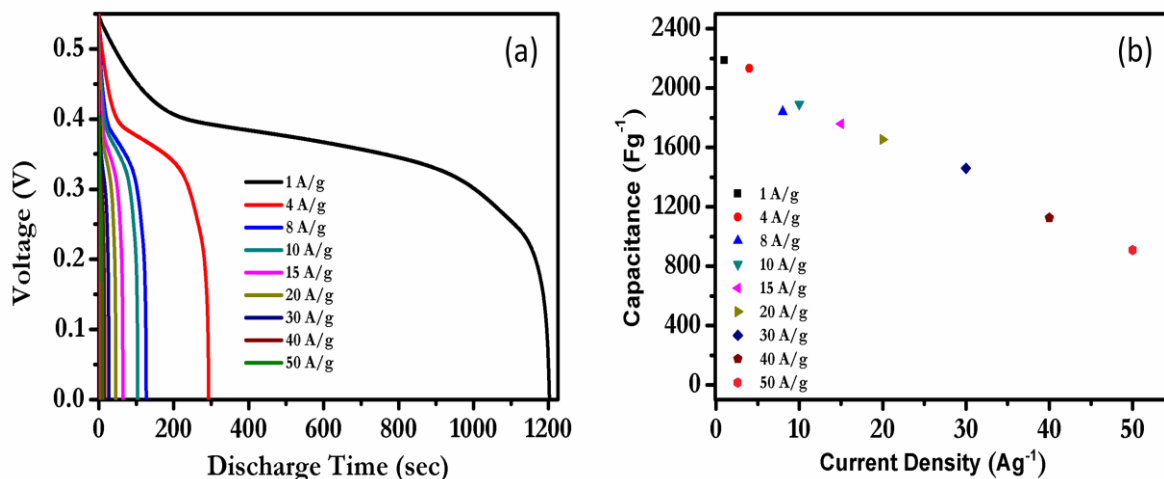
Values of specific capacitance were obtained by using following formula:

$$Cs = I/m \, (\Delta V/\Delta t)$$

Where I is the applied current density, m is the loading of NCS material on the electrode, ΔV is the voltage window and Δt is the discharge time. The specific capacitance values are found to be 2186.36, 2132.72, 1840, 1891, 1759.1, 1654.54, 1459.09, 1127.27, 909.09 F/g at specific current densities of 1, 4, 8, 10, 15, 20, 30, 40 and 50 A/g respectively. These values are higher than most of the other reported Nickel cobalt sulfide nanostructures and also comparable with other reported nanosheet morphology. Detailed comparision table is shown table (3). As mentioned earlier such high capacitance values are a result of long range and thin thickness of the interlocked nanosheet morphology. OH^{-1} insertion and extrusion diffusion pathways are greatly reduced by such interlocked nanosheet morphology, and also large surface area provided by such morphology facilitates high rate capability and a high electrochemical capacitance, which makes it an excellent material for energy storage.

Materials	Capacitance (F/g)	Current Density (A/g)
$Ni_xCo_{3x}S_4$ Hollow Nanoprisms (ref 49)	674	10
$NiCo_2S_4$ urchin (ref 50)	1018	10
$NiCo_2S_4$ nanosheets on graphene (ref 51)	850	10
Ni–Co sulfide nanowires (ref 52)	1627	10
$NiCo_2S_4$ porous nanotubes (ref 53)	2.17 (F/cm^2)	10 (mA/cm^2)
$NiCo_2S_4$ porous nanotubes (ref 54)	933	1
Hollow Hexagonal $NiCo_2S_4$ Nanoplates (ref 55)	437	1
$NiCo_2S_4$ nanosheet (Present Work)	1891	10
$NiCo_2O_4$ Ultrathin Nanosheets on carbon nanofibers (ref 56)	675	10
NiO nanosheet hollow spheres (ref 57)	457	3
Single-Layer β‑$Co(OH)_2$ -graphene (ref 58)	1620	10
Nickel Cobaltite Nanosheets on carbon cloth (ref 59)	191	10
Ultrathin Co_3O_4 nanosheet arrays (ref 38)	1782	5 mA/cm^2

Ultrathin Mesoporous NiCo$_2$O$_4$ Nanosheets (ref 60)	1596	12
Ultrathin Porous NiCo$_2$O$_4$ Nanosheet Arrays (ref 61)	2170	10
Ni-Co oxide nanosheets (ref 62)	1158	10

Table 3: Comparision between various nickel cobalt sulphides morphologies and other reported nanosheet structures

3.4 Conclusion

A 2D porous, uniform folded sheet like morphology of Nickel cobalt sulfide is reported. Its unique feature of large surface area, thin thickness, large range nanostructures and higher conductivity than my previously reported NCO NWs and NCO nanosheets, makes it capacitance much higher. As explained earlier the advantage of long range and thin thickness in increasing the electrochemical performance , higher conductivity by replacing oxygen with sulfur adds up to its capacitance. A very high capacitance of 2183.36 F/g at 1 A/g is obtained from NCS nanosheet. It's a promising material for future energy storage, by not only providing larger power density but also high energy density. The only disadvantage this system might face is its lack of commercial use as it is not synthesized in bulk scale as a powdered form.

With the advancement in science and technology, supercapacitors are advancing in replacing batteries, which takes a lot of time to get charged, besides this shorter life time of batteries makes them unreliable, and also careful measures have to be taken in disposing these old batteries from which harmful chemicals can percolate within the soil and water, making it toxic for humans. Supercapacitors on other hand charge very quickly, they have a longer life span and they are synthesized from non corrosive and non toxic chemicals, making them cleaner and safer. But currently

supercapacitors are facing problems of low energy density than batteries. Supercapacitors can store a large amount of energy but delivers its quickly, it can be effectively used in appliances that require a quick burst of energy, on the other hand batteries have the capability of storing large energy but delivering it slowly making them advantageous over supercapacitors. Hence supercapacitors are facing limitation due to its lower energy density which is only around 1/5 of that of batteries. The use of organic electrolyte in supercapacitors leads to a faster discharge of energy than batteries. Another limitation is that supercapacitors work on low voltages, making them infeasible to be used in commercial electronic devices which work on high voltages. But as said earlier researchers from all over the world are working to make supercapacitors feasible to be used commercially. Scientific breakthroughs have lead scientist to use graphene based supercapacitors, which offer much higher conductivity a faster charging. Placing the electrodes is properly larger surface area of the material could be accessed, which would increase its charge capacity and would have higher rate capability. Some of the researchers are even trying to develop new electrolytes to increase energy storage of the supercapacitors. They are working on preserving charge, while discharging and charging in a very quick time. Scientists are even trying in integrating use of supercapacitors and batteries to jump from existing technology. Hopefully in near future supercapacitors will be made cheaper and smaller and can be used commercially in electronic devices.

References:

[1] Conway, B. E.; Electrochemical Supercapacitors :Scientific Fundamentals and Technological Application, Kluwer-Plenum, *New York*, **1999.**

[2] (a) Hall, P.J.; Mirzaeian, M. S.; Fletcher, I,; Sillars, F. B.; Rennie, A. J. R. ; Bey, G. O. S.; Wilson, G.; Cruden, A.; Carter, R. Energy storage in electrochemical capacitors: designing functional materials to improve performance. Energy Environ. *Sci,* 3, 2**010**, 1238. (b) Naoi, K.; Simon, P. New Materials and New Configurations for Advanced Electrochemical Capacitors. *Electrochem. Soc. Interface*, 34, **2008**,. (c) K€otz, R.; Carlen, M. Principles and applications of electrochemical capacitors. *Electrochim. Acta*, 45, **2000**, 2483.

[3] Brezesinski, T.; Wang, J.; Tolbert, S. H.; Dunn, B. Ordered mesoporous -MoO3 with iso-oriented nanocrystalline walls for thin-film pseudocapacitors .*Nat. Mater,* 9, **2010** , 146 .

[4] Lu, X. H.; Zhai, T.; Zhang, X. H.; Shen, Y. Q.; Yuan, L. Y.; Hu, B.; Gong, L.; Chen, J.; Zhou, J.; Tong, Y. X.; Wang, Z. L. WO3–x@Au@MnO_2 Core–Shell Nanowires on Carbon Fabric for High-Performance Flexible Supercapacitors. *Adv. Mater*, 24, **2012**, 938–944.

[5] Wang, B.; Chen, J. S.; Wang, Z. Y.; Madhavi, S.; Lou, X. W. *Adv. Energy Mater*, 10, **2012**, 1188.

[6] Wei, T. Y.; Chen, C. H.; Chien, H. C.; Lu, S. Y.; Hu, C. C. A Cost-Effective Supercapacitor Material of Ultrahigh Specific Capacitances: Spinel Nickel Cobaltite Aerogels from an Epoxide-Driven Sol–Gel Process. *Adv. Mater*, 22, **2010**, 347.

[7] Wang, Q.; LIU, B.; Wang, X.; Ran, S.; Wang, L.; Chen, Di.; Shen, G. Morphology evolution of urchin-like $NiCo_2O_4$ nanostructures and their applications as psuedocapacitors and photoelectrochemical cells .*J. Mater. Chem*, 22, **2012**, 21647–21653.

[8] Verma, S.; Joshi, H. M.; Jagadale, T.; Chawla, A.; Chandra, R.; Ogale, S. J. Nearly Monodispersed Multifunctional NiCo2O4 Spinel Nanoparticles: Magnetism, Infrared Transparency, and Radiofrequency Absorption.*Phys. Chem. C*, 112, **2008**, 15106.

[9] Marsan, B.; Fradette, N.; Beaudoin, G. Physicochemical and Electrochemical Properties of $CuCo_2O_4$ Electrodes Prepared by Thermal Decomposition for Oxygen Evolution. *J ElectrochemSoc*, 139,**1992,** 1889–1896.

[10] Windisch, CFJ.; Ferris, KF.; Exarches, GJ. Synthesis and characterization of transparent conducting oxide cobalt–nickel spinel films. *J Vac Sci Technol*,19, **2001**, 1647–1651.

[11] Li, Q.; Zeng, L.; Wang, J.; Tang, D.; Liu, B.; Chen, G.; Wei, M. Magnetic Mesoporous OrganicInorganic $NiCo_2O_4$ Hybrid Nanomaterials for Electrochemical Immunosensors *Apply Mater Interfaces*, 3, **2011**, 1366-1373.

[12] Cui, B.; Lin, H.; Li, J. B.; Li, X.; Yang, J.; Tao, J. Core–Ring Structured $NiCo_2O_4$ Nanoplatelets: Synthesis, Characterization, and Electrocatalytic Applications *Adv. Funct. Mater*, 18, **2008,** 1440.

[13] Alcantara, R.; Jaraba, M.; Lavela, P.; Tirado, J. L. $NiCo_2O_4$ Spinel: First Report on a Transition Metal Oxide for the Negative Electrode of Sodium-Ion Batteries. *Chem. Mater*, 14, **2002**, 2847.

[14] Xiao, J. W.; Yang, S. H. RSC Adv, Sequential crystallization of sea urchin-like bimetallic (Ni, Co) carbonate hydroxide and its morphology conserved conversion to porous $NiCo_2O_4$ spinel for pseudocapacitors. *RSC advances*, 1 , **2011** , 588

[15] Wang, H. L.; Gao, Q. M.; Jiang, L. Facile Approach to Prepare Nickel Cobaltite Nanowire Materials for Supercapacitors . *Small*, **2011,** 72454.

[16] Wang, H. X.; Hu, Z. A. ; Chang, Y. Q.; Chen, Y. L.; Wu, H. Y.; Zhang, Z. Y.; Yang, Y. Y. Design and synthesis of $NiCo_2O_4$–reduced graphene oxide composites for high performance supercapacitors. J*. Mater. Chem*, 21, **2011,** 10504.

[17] Cui, B.; Lin, H.; Liu, Y.; Li, J.; Sun, P.; Zhao, XC.; Liu, CJ. Photophysical and Photocatalytic Properties of Core-Ring Structured $NiCo_2O_4$ Nanoplatelets. *J Phys Chem. C*, 113, **2009,** 14083-14087.

[18] Marco, JF.; Gancedo, JR.; Gracia, M.; Gautier, JL.; RmHos, E.; Berry, FJ. *J Solid State Chem,* 153, **2000** , 74–81.

[19] Ding, R.; Li Qi,; Wang, H. Scalable Electrodeposition of Cost-Effective Microsized $NiCo_2O_4$ Electrode Materials for Practical Applications in Electrochemical Capacitors *ECS Electrochem.Lett,* 1,**2012**, A43-A46.

[20] Klissursk, DG.; Uzunova, EL. Synthesis of Nickel Cobaltite Spinel from Coprecipitated Nickel-Co balt Hydroxide Carbonate *Chem Mater*, 3, **1991**, 1060–1063.

[21] Kim, JG.; Pugmire, DL.; Battaglia, D.; Langell, MA. *Appl Surf Sci*, 162, **2000**, 70–84.

[22] Jiang, H.; Ma, J.; Li, C. Z. Hierarchical porous $NiCo_2O_4$ nanowires for high-rate supercapacitorsw *Chem. Commun*, 48 , **2012** , 4465 – 4467.

[23] Zhang, G. Q.; Wu, H. B.; Hoster, H. E.; Chan-Park, M. B.; Lou, X. W. Single-crystalline $NiCo_2O_4$ nanoneedle arrays grown on conductive substrates as binder-free electrodes for high-performance supercapacitors *Energy Environ. Sci*, 5,**2012** , 9453 – 9456.

[24] Kong, L.B.; Lu, C.; Liu, M.C.; Luo, Y.C.; Kang, L. Effect of surfactant on the morphology and capacitive performance of porous $NiCo_2O_4$ *J. Solid State Electrochem.* **2013**, A, 1463-1471.

[25] Wang, H.; Wang, X. Growing Nickel Cobaltite Nanowires and Nanosheets on Carbon Cloth with Different Pseudocapacitive Performance *ACS Appl. Mater. Interfaces*, 5, **2013**, 6255-6260.

[26] Yuan, C.; Li, J.; Hou, L.; Yang, L.; Shan, L.; Zhang, X. Facile template-free synthesis of ultralayered mesoporous nickel cobaltite nanowires towards high-performance electrochemical capacitors *J.Mater.Chem*, 22, **2012**, 16084.

[27] Wang, Q.; Wang, X.; Liu, B.; Yu, G.; Hou, X.; Chen, Di.; shem, G. $NiCo_2O_4$ nanowire arrays supported on Ni foam for high-performance flexible all-solid-state Supercapacitors. *J.Mater.Chem*. A, 1, **2013**, 2468.

[28] Zou, R.; Xu, K.; Wang, T.; He, G.; Liu, Q.; Ziu, X.; Zhang, Z.; Hu, J. Chain-like NiCo2O4 nanowires with different exposed reactive planes for high-performance supercapacitors. *J.Mater.Chem*. A, 1, **2013**, 8560.

[29] Choi, D.; Blomgren, GE.; Kumta, PN. Fast and Reversible Surface Redox Reaction in Nanocrystalline Vanadium Nitride Supercapacitors. *Adv Mater*, 18, **2006**, 1178–1182.

[30] Justin, P.; Meher, SK.; RangaRao, G. Tuning of Capacitance Behavior of NiO Using Anionic, Cationic, and Nonionic Surfactants by Hydrothermal Synthesis. *J Phys.Chem. C*, 114, **2010,** 5203–5210.

[31] Patzke, G. R.; Zhou, Y.; Kontic, R.; Conrad, F. Oxide Nanomaterials: Synthetic Developments, Mechanistic Studies, and Technological Innovations. *Angew. Chem., Int. Ed.,* 50, **2011**, 826.

[32] Whitesides, G. M.; Proc. M.; Boncheva. Beyond molecules: Self-assembly of mesoscopic and macroscopic components *Natl. Acad. Sci. U.S.A.*, 99, **2002**, 4769.

[33] Ding, R.; Qi, Li.; Wang, H. A facile and cost-effective synthesis of mesoporous $NiCo_2O_4$ nanoparticles and their capacitive behavior in electrochemical capacitors. *J. Solid State Electrochem*, 16, **2012,** 3621-3633.

[34] Lu, X. H.; Huang, X.; Xie, S. L.; Zhai, T.; Wang, C. S.; Zhang, P.; Yu, M. H.; Li, W. ; Liang, C.L.; Tong, Y.X. Controllable synthesis of porous nickel–cobalt oxide nanosheets for supercapacitors. *J. Mater. Chem*, **2012**, 22,13357.

[35] Gupta, V.; Gupta, S.; Miura, N. Electrochemically synthesized nanocrystalline spinel thin film for high performance supercapacitor.*J. Power Sources*, 195, **2010**, 3757.

[36] Zhang, G. Q.; Lou, X. W. Controlled growth of $NiCo_2O_4$ nanorods and ultrathin nanosheets on carbon nanofibers for high-performance supercapacitors. *Sci. Rep.*, 3, **2013,** 1470.

[37] Wu, Y. Q.; Chen, X. Y.; Ji, P. T.; Zhou, Q. Q.; Sol–gel approach for controllable synthesis and electrochemical properties of $NiCo_2O_4$ crystals as electrode materials for application in supercapacitors . *Electrochim. Acta*, 56, **2011,** 7517.

[38] Yang, Q.; Lu, Z.; Sun, X.; Liu, J. Ultrathin Co_3O_4 nanosheet arrays with high supercapacitive performance. *Scientific Reports*, 3, 3537, **2013**

[39]. Meher, S. K. & Rao, G. R. Ultralayered Co_3O_4 for High-Performance Supercapacitor Applications. *J. Phys. Chem. C* 115, 15646–15654 (**2011**).

[40]. Hsu, Y.-K.et al. Reversible phase transformation of MnO_2 nanosheets in an electrochemical capacitor investigated by in situ Raman spectroscopy. *Chem. Commun* 47, 1252–1254 (**2011)**.

[41] Xia, X-h.; Tu, J-p.; Mai, Y-j.; Wang, X.-l.; Gu, C-d.; Zhao, X-b. Self-supported hydrothermal synthesized hollow Co_3O_4 nanowire arrays with high supercapacitor capacitance. *J. Mater. Chem.*, **2011**, 21, 9319–9325.

[42] Zhong, J-H.; Wang,A-L.; Li, G-R.; Wang, J-W.; Ou, Y-N.; Tong, Y-X. Co_3O_4/Ni(OH)$_2$ composite mesoporous nanosheet networks as a promising electrode for supercapacitor applications. *J. Mater. Chem.*, **2012**, 22, 5656.

[43] Zhu, T.; Chen, J. S.; Lou, X. W. Shape-controlled synthesis of porous Co_3O_4 nanostructures for application in supercapacitors *J. Mater. Chem.*, **2010**, 20, 7015.

[44] Zhu, T.; Wang, Z.; Ding, S.; Chen, J.S.; Lou, X. W. (D.). Hierarchical nickel sulfide hollow spheres for high performance supercapacitors. *RSC Adv.*, **2011**, 1, 397.

[45] Zhang, L.; Wu, H. B.; Lou, X. W. (D.). Unusual CoS_2 ellipsoids with anisotropic tube-like cavities and their application in supercapacitors. *Chem. Commun.*, **2012** ,48, 6912

[46] Wei,T-Y.; C-H. Chen,; Chien, H-C.; Lu, S-Y.; Hu, C-C. A Cost-Effective Supercapacitor Material of Ultrahigh Specific Capacitances: Spinel Nickel Cobaltite Aerogels from an Epoxide-Driven Sol–Gel Process. *Adv. Mater.*, **2010**, 22, 347

[47] Zhang ,G.; Lou, X. W. (D.). General Solution Growth of Mesoporous $NiCo_2O_4$ Nanosheets on Various Conductive Substrates as High-Performance Electrodes for Supercapacitors. *Adv. Mater.*, **2013**, 25, 976

[48] Chen, H.; Jiang, J.; Zhang, L.; Wan, H. Qi, T.; Xia, D. DOI: 10.1039/b000000x

[49] Yu, L.; Zhang, L.; Wu, H. B.; (David) Lou, X.W. Formation of $Ni_xCo_{3\_x}S$ Hollow Nanoprisms with Enhanced Pseudocapacitive Properties. *Angew. Chem.* **2014**, 126, 1 – 5.

[50] Chen, H.; Jiang, J.; Zhang, L.; Wan, H.; Qi, T.; Xia, D. Highly conductive $NiCo_2S_4$ urchin-like nanostructures for high-rate pseudocapacitors. *Nanoscale*, **2013**, 5, 8879.

[51] Peng, S.; Li, L.; Li, C.; Tan, H.; Cai, R.; Yu, H.; Mhaisalkar, S.; Srinivasan, M.; Ramakrishna, S.; Yan, Q. In situ growth of $NiCo_2S_4$ nanosheets on graphene for high-performance supercapacitors. *Chem. Commun.*, **2013,** 49, 10178.

[52] Li, Y.; Cao, L.; Qiao, L.; Zhou, M.; Yang, Y.; Xiao, P.; Zhang, Y. Ni–Co sulfide nanowires on nickel foam withultrahigh capacitance for asymmetric supercapacitors. *J. Mater. Chem.* A DOI: 10.1039/c3ta15373h

[53] Xiao, J.; Wan, L.; Yang, S.; Xiao, F.; Wang, S. Design Hierarchical Electrodes with Highly Conductive $NiCo_2S_4$ Nanotube Arrays Grown on Carbon Fiber Paper for High- Performance Pseudocapacitors. *Nano Lett.* **2014**, 14, 831−838.

[54] Wan, H.; Jiang, J.; Yu, J.; Xu, K.; Miao, L.; Zhang, L.; Chen, H.; Ruan, Y. $NiCo_2S_4$ porous nanotubes synthesis via sacrificial templates: high-performance electrode materials of supercapacitors. *CrystEngComm*, **2013,** 15, 7649.

[55] Pu, J.; Cui, F.; Chu, S.; Wang, T.; Sheng, E.; Wang, Z. Preparation and Electrochemical Characterization of Hollow Hexagonal $NiCo_2S_4$ Nanoplates as Pseudocapacitor Materials. *ACS Sustainable Chem.* Eng.dx.doi.org/10.1021/sc400472z.

[56] Zhang, G.; (David) Lou, X.W. Controlled Growth of $NiCo_2O_4$ Nanorods and Ultrathin Nanosheets on Carbon Nanofibers for High-performance Supercapacitors. *SCIENTIFIC REPORTS* ,**2013**, 3,1470.

[57] Ding, S.; Zhu, T.; Chen, J.S.; Wang, Z.; Yuan, C.; (David) Lou, X W. Controlled synthesis of hierarchical NiO nanosheet hollow spheres with enhanced supercapacitive performance. *J. Mater. Chem.*, **2011,** 21, 6602.

[58] Wang, L.; Lin, C.; Zhang, F.; Jin J. Phase Transformation Guided Single- Layer ƒÀ.$Co(OH)_2$ Nanosheets for Pseudocapacitive Electrodes. *ACS Nano*, DOI 10.1021/nn500386u.

[59] Wang, H.; Wang, X. Growing Nickel Cobaltite Nanowires and Nanosheets on Carbon Cloth with Different Pseudocapacitive Performance. *ACS Appl. Mater.* Interfaces **2013**, 5, 6255−6260.

[60] Yuan, C.; Li, J.; Hou, L.; Zhang, X.; Shen, L.; (David) Lou, X.W. Ultrathin Mesoporous $NiCo_2O_4$ Nanosheets Supported on Ni Foam as Advanced Electrodes for Supercapacitors. *Adv. Funct. Mater.* **2012**, 22, 4592–4597.

[61] Du, J.; Zhou, G.; Zhang, H.; Cheng, C.; Ma, J.; Wei, W.; Chen.; Wang, T.

Ultrathin Porous $NiCo_2O_4$ Nanosheet Arrays on Flexible Carbon Fabric for High-Performance Supercapacitors. *ACS Appl. Mater. Interfaces,* **2013,** 5, 7405−7409.

[62] Wang, R.; Yan, X. Superior asymmetric supercapacitor based on Ni-Co oxide nanosheets and carbon nanorods. *SCIENTIFIC REPORTS* , **2013,**4, 3712.